HERON contains contributions based mainly on research work performed in I.B.B.C. and STEVIN and related to strength of materials and structures and materials science.

Jointly edited by:

STEVIN-LABORATORY
of the Department of Civil Engineering of the Technological University, Delft, The Netherlands
and
I.B.B.C. INSTITUTE TNO
for Building Materials and Building Structures, Rijswijk (ZH), The Netherlands.

HERON vol. 17
1970-'71
no. 4

Contents

The stability of doubly curved shells having a positive curvature index

A. M. Haas
Technological University, Delft

H. van Koten
T.N.O., Applied Scientific Research, Delft

PREFACE

The post-war development of shell theory has resulted in a large extension of the field of application – especially in the area of doubly curved shells.

The phantastic progress of thin metal shells in mechanical and aeronautical engineering is well-known. The large development in airplane techniques and missible projects has partly been made possible by profound research in shell problems.

In building construction a similar trend can be traced. No longer was the application restricted to the domes and the various types of cylindrical shells. One may also observe the application of shell structures in a wider range of spans. And with it came the demand for spatial structures covering large areas unobstructed by columns. As many of these shells were built of reinforced concrete the specific characteristics of this material also played a role. As spans grew and the column-free areas became larger, the question of the stability of the shell structure became of paramount significance. Asked for a stability-criterion the reply was given to apply a somewhat higher factor of safety than is applicable for steel. And this period is not yet closed!

The cases when the structural engineer was confronted with these problems became more and more frequent, although knowledge and insight did not increase proportionally. One has only have to be confronted with or to read the publications concerning shell structures of the post-war period to find that the final problem ends (or rather starts) with the question of the stability.

Reference is made to the general Report on the instability of prestressed shells by Prof. Franco Levi, F.I.P. Congres Amsterdam (1955). And to the shell roof of the Industry Palace at Paris, respectively to the north-light shells of the factories at Oosterhout (Holland). It may explain the urge felt by the authors to study the matter more profoundly in order to gain more insight and to be better equipped.

Starting in 1963 they set out on two paths: a critical review of the basic theory respectively a new approach of safety criteria for concrete shells. And the latter to be accompanied by research.

Chapter II and III are specimen of the path they first followed; it resulted in publications at Budapest (IASS, 1965) and at Leningrad (IASS, 1966). They based themselves on the method followed by Von Kármán and Tsien, thereby introducing different boundary conditions and an elliptic shape of the snap-through area.

The new approach resulted in a critical review of the classic criteria. First of all it meant the introduction of the non-linear property of concrete. Attention was therefor essentially shifted to the critical strain thereby eliminating the fluctuating value of the modulus of elasticity of concrete.

A new concept of the buckling problem is based on the observation of the configurations of equilibrium in the vicinity of the critical stress. As soon as the stability-limit is reached the shell must snap into another configuration. This is a procedure developed and published by Koiter. If transferred into a strain criterion this comfiguration (indicated by a parabolae for a cylindrical shell) will present the boundary for the critical instability strain.

Another approach occupies itself with the buckling pattern of thin concrete shells. It already was evident that a comparison of the instability behaviour between concrete and thin steel cylindrical shells fails. The buckling pattern of thin steel cylinders does not appear. To that end a dozen reinforced concrete cylindrical shells were tested. Due to the rather large value of the ratio t/R the instability boundary was not reached and failure apparently took place as a result of reaching the crushing strength. Nevertheless from these investigations it appeared that the reinforcement in the shallow concrete shell does not seem to be decisive for the behaviour. Nor do imperfections of the shape which in the stability research of metal shells play an important role, have much influence in practical application.

On account of the brittle failure observed and relying on preliminary conclusions that it is the material concrete that is decisive in the stability behaviour, the next step was a check on the stability boundary of cylindrical shells of plastic material. The investigations of four cylinders resulted in a fair coincidence with the mentioned strain boundary.

These observations will be the subject of a second publication. Finally the authors endeavour to extend these concepts into the entire field of thin concrete shells, compromising the negative curvatures index ones (hyppars, etc.) as well.

A first incitative can be found under the heading of specific cases in this contribution. There an attempt has been made to include the transition into singly curved phenomenae.

In the third publication will be included the results of the stability tests on doubly curved thin concrete shells, which are already in the course of preparation.

Notations

A snap-through area

A_1 $-\dfrac{l}{a_1^4+6a_1^2b_1^2+b_1^4}$

a_1 half long axis of elliptic snap-through-area

α parameter of load distribution

α parameter in buckling formula

α_1 coefficient of the edge-beam stiffness

A, B parameters used in the calculation of the edge disturbance

B dimension of edge-beam

b B/t

b_1 half short axis of elliptic snap-through-area

c radius at snap-through-area

γ $q/E(t^2/R_2^2)$, dimensionless load-factor

E modulus of elasticity

F $Ef(f-b_1^2/R_2)$

f rise of snap-through-area

φ angle

Φ stress function

ϕ f/t

H dimension of edge-beam

h H/t

ϑ half of the angle of aperture

ψ $b_1/(\sqrt{R_2 t})$ (for the sphere $c/\sqrt{Rt}$)

λ parameter (for the sphere being $\sqrt[4]{3}/\sqrt{Rt}$)

parameters used in the calculation

π 3,1416

q radial load

R radius in general

R_1, R_2 principal radius of curvature

r radius in general (chapter I)

r ordinate in snap-through-area

σ stress

t shell thickness

U energy

U_m strain energy due to stretching of the middle plane of the shell

U_b strain energy due to bending

U_g energy due to external loads

w radial deflection

w_0, x_0, y_0 coördinates of a point of the edge of the snap-through-area

THE STABILITY OF DOUBLY CURVED SHELLS HAVING A POSITIVE CURVATURE INDEX

Summary

Post-war development of shell theory and research resulted in a large extension of the field of application, especially in the area of doubly curved shells. It had its influence on building construction as well. An application of shell structures in a wide range of spans can be observed; with it came the demand for spatial structures covering areas unobstructed by columns. Thus the question of the stability became of paramount importance.

In studying the matter the authors have reviewed the classic criteria. For the positive curvature-index they introduced a somewhat different assumption for the shape of the snap-through-area. Moreover the problem could be extended from the spherical dome into an elliptic surface.

Furthermore the influence of the edge stiffness was studied, employing energy considerations. Introducing a number of assumptions the authors could arrive at a first approximation to be used in study and design. Thereby the degree of stiffness of the edge-beam was varied. A numerical example is added.

This publication can be seen as a critical compilation of the contributions given (and later published in the Proceedings) of the IASS Symposium at Budapest (1965) and at the Congress of Leningrad (1966).

DE STABILITEIT VAN DUBBEL-GEKROMDE SCHALEN MET EEN POSITIEVE KROMMINGSMAAT

Samenvatting

De na-oorlogse ontwikkeling van de theorie en het onderzoek van schalen heeft tot een grote verbreiding van het veld van toepassing geleid, in het bijzonder ten aanzien van de dubbel-gekromde schalen. Het had zijn invloed op de bouwconstructies. Een gevolg was ook de toepassing voor schalen van grotere overspanningen. Daarbij aansluitend kwam de vraag naar ruimtelijke constructies, die oppervlakkten waarin geen kolommen voorkomen moeten overdekken. Aldus werd het vraagstuk van de stabiliteit van groot belang.

In hun studie hebben de schrijvers de klassieke maatstaven in beschouwing genomen. Voor de positieve krommingsmaat werd een ietwat andere vorm van het doorslaggebied verondersteld. Bovendien kon het probleem van de doorslag van een bolschaal ook worden betrokken op een elliptisch oppervlak.

Voorts werd de invloed van de randverstijving bestudeerd door gebruik te maken van energie-overwegingen. Door het invoeren van een aantal aannamen konden de schrijvers komen tot een eerste benadering, die dienst kan doen voor verdere studie en voor een ontwerp. Daarbij werd de stijfheid van de randbalk variabel gesteld. Een rekenvoorbeeld werd toegevoegd.

Deze publikatie kan worden opgevat als een kritische compilatie van de bijdragen gegeven (en later gepubliceerd in de desbetreffende verhandelingen) ter gelegenheid van het IASS-Symposium te Budapest (1965) en van het Congres te Leningrad (1966).

The stability of doubly curved shells having a positive curvature index

I Introduction

In an introduction to a subject on stability, the name of Euler – famous for his concept – should not be omitted. He developed the behaviour of a bar under axial load and even investigated it after the buckling load was exceeded. It took about one century and a half before an extension into the domain of plates was effectuated, and only in our age the investigation of the stability of shells took place. In the beginning it was wholly confined to the behaviour of singly curved viz. cylindrical shells.

It is a logical and comprehensive procedure to develop these stability considerations in stages, each time stepping up a dimension. The sequence here indicated may in short be named as: bar, plate, shell. Another also valuable order can in short be termed as: bar, arch, shell. Nevertheless which sequence is followed, one is faced with additional problems not only related to another dimension but greatly increasing the mathematical analysis involved, especially for the three-dimensional shell elements. In this respect the treatment has more and more departed from the usual analysis in applied mechanics when design is concerned with the solution of problems of change (deformation) under the action of forces, as well as the solution of problems of failure of critical parts (sections) of the systems. It turned to the application of the energy-method. In these cases of shells it was found the most adaptable method to apply in regard to the increasing complexity of the problem.

Still another fundamental problem should be looked into.

If restricted to shallow spherical shells the present situation is rather succinctly. On the basis of the linear theory Zoelly [1] developed in 1915 his buckling-formula for a spherical dome. Experimental values range from about 10 to about 50% of the theoretical value. In large part this defect is thought to be due to regressive behaviour after buckling affected by inherent initial imperfections of form. And also by imperfection introduced by the elastic deformation of the partial shell together its edges prior to buckling. Theoretical analysis has gone some way towards quantitative estimation of these effects and some measure of agreement with the experimental values has been achieved. In this respect the solution of Von Kármán, Tsien, Mushtari and Feodosjew should be mentioned.

Energy criterion

An effective starting point is the investigation into the stability of a state of equilibrium. Such a state can only be stable if the potential energy is a minimum. In first instance it will be considered for a small displacement and only the quadratic terms will be involved. If the sum of these terms will always be positive, then the equilibrium

is said to be stable. If the sum can also assume negative values then the equilibrium is unstable. On the boundary of stability-problems the sum-total will be zero for an appropriate value of the displacement. For this case a stress, the critical buckling-stress can be calculated including the buckling shape. For shells when limiting to quadratic terms, it means the neglect of the modification of the curvature radius due to the deformation.

Now in short the application of the energy principles will be treated for the sequence bar-plate-shell.

Bar

For a bar axially loaded by compression the increase of the elastic energy per unit-length due to bending equals:

$$\frac{EI}{2}\left(\frac{\mathrm{d}^2w}{\mathrm{d}x^2}\right)^2$$

if the cross-section measures b.h. In this expression w denotes the lateral deflection and E the modulus of elasticity. The increase of bending energy per unit of volume of the bar can be expressed as:

$$\frac{\mathrm{d}U}{\mathrm{d}V} = \tfrac{1}{2}\sigma\varepsilon = \tfrac{1}{2}\frac{\sigma^2}{E}.$$

Substituting $\sigma = Mz/I$ and again for $M = -\varrho EI$, the expression for σ will be:

$$\sigma = \frac{\mathrm{d}^2w}{\mathrm{d}x^2}Ez, \rightarrow \text{if } -\varrho = \frac{\mathrm{d}^2w}{\mathrm{d}x^2}$$

Then can be written:

$$\frac{\mathrm{d}U}{\mathrm{d}V} = \tfrac{1}{2}E^2z^2\left(\frac{\mathrm{d}^2w}{\mathrm{d}x^2}\right)^2 \cdot \frac{1}{E} = \tfrac{1}{2}E\left(\frac{\mathrm{d}^2w}{\mathrm{d}x^2}\right)^2 z^2.$$

Integrated for a cross-section:

$$\frac{E}{2}\left(\frac{\mathrm{d}^2w}{\mathrm{d}x^2}\right)^2 \int_A z^2\mathrm{d}A = \frac{EI}{2}\left(\frac{\mathrm{d}^2w}{\mathrm{d}x^2}\right)^2$$

and considered the total l the total strain energy will be:

$$\frac{EI}{2}\int_0^l \left(\frac{\mathrm{d}^2w}{\mathrm{d}x^2}\right)^2 \mathrm{d}x$$

On the other hand there is work done by the external forces. In this case it is negative since the displacement u and the force P have the same direction: $T = -Pu$. The displacement u depends on the deflection w and since we need energy terms which are quadratic, we should have the relation between u and w related to a term expressed in w^2.

In the deflected state (fig. 1) the element dx is measured on the curved axis. It makes an angle dw/dx with the vertical and its vertical projection is:

$$dx \cos \frac{dw}{dx} = dx \left[1 - \tfrac{1}{2} \left(\frac{dw}{dx} \right)^2 + \dots \right].$$

The sum of these projections equals: $l - v$.

Up to the second-order term

$$l - v = \int_0^l \left[1 - \tfrac{1}{2} \left(\frac{dw}{dx} \right)^2 \right] dx = \int_0^l dx - \tfrac{1}{2} \int_0^l \left(\frac{dw}{dx} \right)^2 dx; \text{ whence } U = \tfrac{1}{2} \int_0^l \left(\frac{dw}{dx} \right)^2 dx.$$

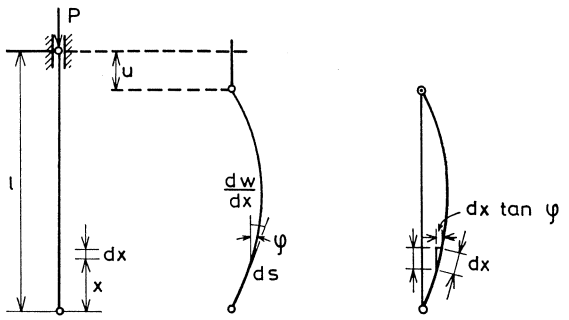

Fig. 1.

For details one is referred to Flügge; or to Haas [9].

Thus the total energy needed to produce the deflection w is:

$$\frac{EI}{2} \int_0^l \left(\frac{d^2w}{dx^2} \right)^2 dx - \frac{P}{2} \int_0^l \left(\frac{dw}{dx} \right)^2 dx$$

If this equation is zero, the value of the critical load P is found. Looking at the quotient:

$$P = \frac{EI \int_0^l \left(\frac{d^2w}{dx^2} \right)^2 dx}{\int_0^l \left(\frac{dw}{dx} \right)^2 dx},$$

the numerator as well as the denominator are quadratic in derivatives of w. Then the quotient does not depend on the absolute magnitude of w, but on its distribution. We want to find that special distribution $w = w(x)$ which yield the smallest value of P: P_{cr}.

There are different ways of arriving at the smallest value. We may take the well-known different equation:

$$EI\frac{d^2w}{dx^2} + Pw = 0,$$

and solve it and discuss the solution; thereby considering the boundary conditions.

Another way is to assume a very general expression for $w(x)$. Usually a Fourier series is chosen of the form

$$w(x) = \sum C_n \sin\frac{n\pi x}{l}$$

which has to satisfy the boundary conditions. Then the coefficients are determined so that P becomes a minimum. It is then found that $C_n = 0$ for $n > 1$; and that C_1 is arbitrary, while P becomes the equal to the Euler load:

$$P = \frac{EI\pi^2}{l^2}$$

It is an asset of the energy method that it allows finding approximate values of P_{cr} by introducing some plausible functions $w(x)$. Since this is not necessarily the one which makes P a minimum, the approximate value of P is always higher than the correct one. The P_{cr} is an upper bound solution. The choice of a function $w(x)$ which approximates the real buckling form has the tendency to somewhat stiffer the system. Therefore, the result is not on the safe side. However it usually comes close to the correct one if the function $w(x)$ is skilfully chosen.

The reason why this is mentioned somewhat at length is that for the problems to be encountered in later chapters (on shells) this approach will be the only way to arrive at a solution, which, as explained, should be observed with some caution.

Summarizing for a prismatic bar having hinges at both ends, the expression for the increase of the potential energy equals:

$$U = \int_0^l \left[\tfrac{1}{2}EI\left(\frac{d^2w}{dx^2}\right)^2 - \tfrac{1}{2}\sigma A\left(\frac{dw}{dx}\right)^2\right]dx$$

This increase is always positive for

$$\sigma < \sigma_{cr} \quad \text{if} \quad \sigma_{cr} = \frac{\pi^2 E^2 I}{l^2}$$

For this critical stress the buckling form will be:

$$w = a\sin\frac{\pi x}{l}$$

in which a denotes an arbitrary amplitude.

If for the bar is taken a strip or a plate with cross-section $A = bt$, then we can write:

$$I = \frac{bt^3}{12} \quad \text{and} \quad P = \sigma bt.$$

Consequently the expression for the potential energy will be:

$$U = \int_0^l \left(\frac{1}{24} Ebt^3 \left(\frac{\mathrm{d}^2 w}{\mathrm{d}x^2} \right)^2 - \tfrac{1}{2}\sigma bt \left(\frac{\mathrm{d}w}{\mathrm{d}x} \right)^2 \right) \mathrm{d}x$$

With the critical stress $\sigma_{cr} = P_{cr}/bt$ it is now written as

$$\sigma_{cr} = \frac{\pi^2 E t^2}{12 l^2}$$

Plate

For a flat rectangular plate loaded in its middle plane in the x-direction the increase of energy due to the bending of the plate amounts to:

$$\tfrac{1}{2} \frac{EI}{1-\nu^2} \left(\frac{\partial^2 w}{\partial x^2} + \frac{\partial^2 w}{\partial y^2} \right)^2$$

per unit of surface.

If adapted to the plate-notations we write:

$$\frac{Et^3}{24(1-\nu^2)} \left(\frac{\partial^2 w}{\partial x^2} + \frac{\partial^2 w}{\partial y^2} \right)^2$$

This refers to a plate fixed and supported at four sides. The available energy will be – before buckling – diminished by the compressive stress σ to an amount of $\frac{1}{2}\sigma t(\partial w/\partial x)^2$ per unit of surface. Thus the total energy will be

$$U = \iint \left[\frac{Et^3}{24(1-\nu^2)} \left(\frac{\partial^2 w}{\partial x^2} + \frac{\partial^2 w}{\partial y^2} \right)^2 - \tfrac{1}{2}\sigma t \left(\frac{\partial w}{\partial x} \right)^2 \right] \mathrm{d}x \mathrm{d}y,$$

if integrated over the entire plate surface.

For a plate $l \cdot b$ supported on all sides by means of hinges, if l is a multiple of b, or if $l \gg b$ the critical stress will be (fig. 2):

$$\sigma_{cr} = \frac{\pi^2 E t^2}{3(1-\nu^2) b^2}$$

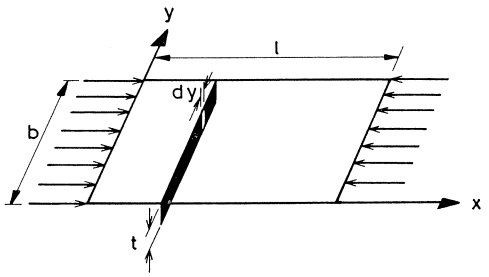

Fig. 2.

The deflection function belonging to it is:

$$w = a \sin \frac{\pi x}{b} \sin \frac{\pi y}{b}$$

Shell

For an axially loaded cylindrical shell (fig. 3) the stability due to compression will be observed, assuming an axial symmetrical buckling-form having a radial displacement w. The bending energy can be expressed in two terms, the first one being

$$\frac{Et^3}{24(1-\nu^2)}\left(\frac{\partial^2 w}{\partial x^2}\right)^2$$

and the second related to the specific elongation in the direction of the circumference.

This specific elongation in the direction of the circumference (ring) equals to w/r, belonging to a radial displacement w.

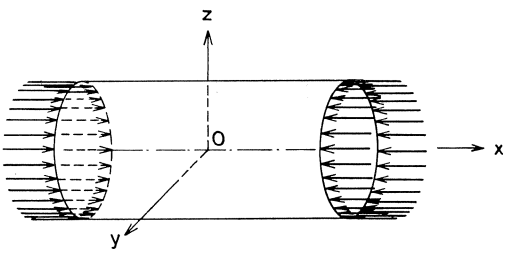

Fig. 3.

If there are axial deformations as well, and in such way that the axial strain equals ν times the specific elongations in the direction of the circumference (ring) the energy-increase will be the smallest, and can be expressed as

$$\tfrac{1}{2}\sigma\varepsilon = \tfrac{1}{2}E\varepsilon^2 = \frac{Ew^2}{2r^2}$$

The decrease of the energy before buckling, will again be:

$$\tfrac{1}{2}\sigma t\left(\frac{\partial w}{\partial x}\right)^2$$

Thus the total increase of the energy will be:

$$U = 2\pi r \int\left[\frac{Et^3}{24(1-\nu^2)}\left(\frac{\partial^2 w}{\partial x^2}\right)^2 + \frac{Et}{2r^2}w^2 - \tfrac{1}{2}\sigma t\left(\frac{\partial w}{\partial x}\right)^2\right]\mathrm{d}x$$

The integral covers the whole surface; the term $2\pi r$ refers to the multiplier in the ring direction. If the cylinder is not too short or in case the edges are adequately supported the introduction of boundary conditions can be abandoned. It means that away from the supports, the buckling pattern can be described by $\cos px/r$ with an arbitrary wave number p.

The increase of energy is positive for

$$\sigma < \frac{p^2Et^2}{12(1-\nu^2)r^2} + \frac{E}{p^2},$$

having a minimum value:

$$\sigma = \frac{Et}{r\sqrt{3(1-\nu^2)}}$$

for a symmetrical buckling form. This value is also found for an unsymmetrical form where w will be a function of both coordinates x and y. They can be described by

$$w = \begin{matrix}\cos\\ \sin\end{matrix}\left(\frac{px}{r}\right)\begin{matrix}\cos\\ \sin\end{matrix}\left(\frac{ny}{r}\right)$$

in which p and n are the wave numbers. For the derivation of the minimum use is made of the relationship between both.

From the foregoing energy-equations for the shell respectively for the plate, and from the subsequent expressions of the critical buckling stress there exists a striking difference between the flat plate and the shell. For the latter the critical stress appears to be linear to the relation t/r, whereas for the plate the relation is quadratic to t/b; having in mind that l is a function of b. Only for very small values of t/r the critical stress will be below the proportional limit of the material. In common words it may be stated that the buckling load of a cylindrical shell differs from that of a comparable sized plate. The cause of the much higher critical stress apparently lies in the middle

term of the expressions for the increase of energy due to the deformation of the middle plane. A corresponding term lacks in the expression of the plate.

Thus term $Et/2(w/r)^2$ will always be present in the case of a closed shell of positive curvature and also for a cylindrical shell being firmly supported at its ends. It indicates the impossibility of such a closed surface to be subjected to an infinitesimal displacement without a deformation of the surface itself. Indeed the cylinder is a developable surface and therefore cannot be turned into a non-developable one.

In the case of a partial cylinder (fig. 4) the curved middle plane does not find sufficient support at the free edges. Due to absence of restraint edges, finite deformation of the edges will occur sooner and the restraint offered to the radial deformations will be far less than for a complete cylinder; inextensional deformations will take place and a relatively small buckling load may be expected.

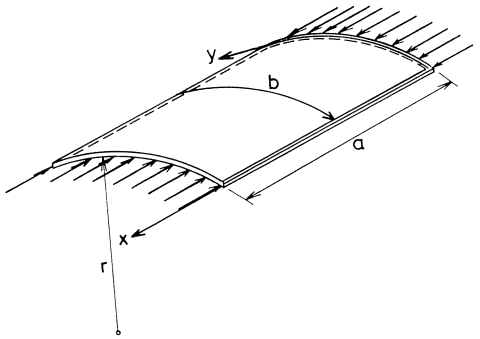

Fig. 4.

The discussed property of a developable surface essentially is confined to an infinitesimale distortion of the shell. If displacements of finite magnitude are allowed, it appears possible to choose these displacements in such a way that the deformed surface will be developable. This is the case for a rhombic or diamond-shaped pattern which has been observed during many tests on this walled cylinders. Examples are: the result of maximum loading of a thin metal cylinder; a model made of paper in which the mentioned pattern has been simulated by the applicance of large folds.

There are circumstances under which another buckling pattern, known as the "concertina", occurs. Although it fits into the general reasoning no special attention will be given to it. This buckling pattern can be taken as a composition of approximately flat plates intersecting at yield-lines which function as ribs.

For plates a lower energy-level is valid. In the parts adjacent to the ribs bending will occur, which means an addition of bending-energy. The total potential energy will depend on the buckling pattern in regard to size and shape. The rotational capacity of the intersecting planes at the rib will also play a role.

In Russian literature much attention is given to the study of the geometry of the post-buckling pattern and to an approach which makes use of this study in order to deduct the critical load.

To this mechanical explanation mathematical observations should be added. If the region of the infinitesimal deformations is exceeded the (middle) term related to the membrane energy, will vanish. This can also be stated in another way: the buckling occurs before the Euler load is reached. The latter belongs to the state of elasticity. There appears to be another way out: a snap-through which consumes less energy. The existance of configurations with a lower level of energy makes it understandable that arbitrary disturbancies, for instance small deviations of the ideal shell form, will result in a transition to such lower level.

A non-linear buckling-theory must be apply to these cases of finite deformations. To try and obtain an exact and complete solution is hardly impossible. One should be satisfied with approximations and trust that these will represent the reality sufficiently. A wellknown method is the one developed by Von Kármán and Tsien [2]. Making use of the stress function of Aery they succeeded to derive (in 1941) two coupled differential equations for shallow shells of the closed cylindrical type.

An approximated solution could be given by choosing a tractable function of the deflection w having a number of free parameters in it. The result of the calculations is shown in figure 5 where the difference in behaviour, the values of buckling in the linear as well as in the non-linear regions can be observed. The stresses are presented as a function of the axial strain; here the non-dimensional values of σ/σ_{cr} are plotted against the values of $\varepsilon/\varepsilon_{cr}$. σ_{cr} and ε_{cr} are the critical buckling stresses respectively strains.

In the elastic region the behaviour is indicated by the straight line OA (*a*). After buckling the relation as found from experiments is given by the line *b*. Initially this line closely follows *a*. Then two courses may occur, indicated by b_1 and b_2. Also the

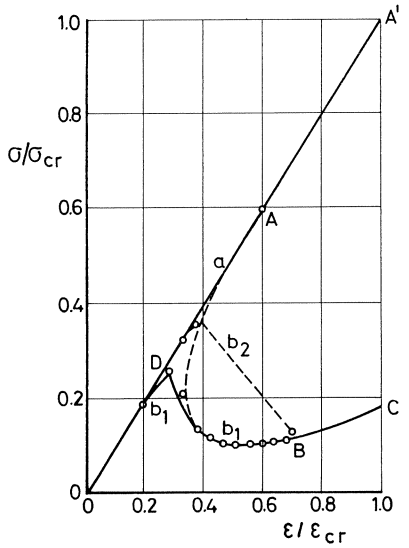

Fig. 5.

finite deformation may already appear at D and then follow the line b_1. Or when the deviation appears at a later stage and then follows the lines b_1 or b_2.

It is clear that the point A′ is never reached. After the snap-through the paths followed can be indicated by curves A–B. Thereafter there will be an inclined curve suggesting a somewhat stable behaviour.

Our interest goes chiefly to the minimum value which will be found somewhere on the curve A–B, or at the point B. In 1954 Kempner [3] deduced a theoretical value of 0.3 for the ratio $(\sigma/\sigma_{cr})/(\varepsilon/\varepsilon_{cr})$. Later when computor-techniques developed and possibilities were created to handle much more equations, a ratio of 0,1 was reached by Amroth (1963); 11 free parameters were used. Later by carefully executed tests on aluminium cylinders, a value of 0.1 was found as well. The result is that there is a reasonable agreement between the theoretical approach and the experiments. The course of curve A–B as well as the inclined branch after B do agree satisfactorily. Also Donnell and Wan by introducing initial imperfections into the non-linear problems, could better explain the apparent discrepancies between empirical and theoretical values.

When there exists initial imperfection, a snap-through buckle occurs earlier than for the perfect cylinder. The emperical relation deviates at point D and begins to follow curve b_1. However the minimum value found, differs only a trifle from the one which is found when the buckling occurs at a later stage.

Deviations from the exact shape may easily be of the order of the shell thickness. This statement made by Flügge, probably holds true for metal cylinders. For concrete ones it generally will be less. As will be reported later on in this contribution the deviations for concrete cylinders prove to be far less.

Doubly curved shells

For the application of a non-linear theory of stability the buckling shape has been formulated by a collection of curves indicated by the formulae

$$w = \begin{matrix}\cos \\ \sin\end{matrix}\left(\frac{px}{r}\right)\begin{matrix}\cos \\ \sin\end{matrix}\left(\frac{ny}{r}\right)$$

For an arbitrary choice of the buckling shape the amount of energy can be calculated thereby including the quadratic terms, cubic ones, etc. if necessary.

As a starting point for the doubly curved shell positive curvature index, the classical shape, the spherical shell was firstly chosen. The spherical dome loaded by a uniform radial pressure q is characterized by a compressive stress in all normal cross-sections of $\sigma = qr/2t$, in which r is the radius. In the linear form the buckling-problem has been solved by Zoelly (1915), the critical stress being:

$$\sigma_{cr} = \frac{1}{\sqrt{3(1-\nu^2)}} E\frac{t}{r}; \quad \text{for } \nu = 0.3 \text{ (steel)} \quad \sigma_{cr} = 0.605E\frac{t}{r}$$

$$\text{for } \nu = 0.2 \text{ (concrete)} \quad \sigma_{cr} = 0.58E\frac{t}{r}$$

The relation between the pressure and the stress being:

$$\sigma = \frac{qr}{2t} \quad \text{or} \quad q = \frac{2\sigma t}{r}$$

the formulae for the buckling load can be written as:

$$q_{cr} = \frac{2}{\sqrt{3(1-\nu^2)}} E\left(\frac{t}{r}\right)^2$$

and again differentiating for steel and for concrete:

$$\nu = 0.3 \qquad q_{cr} = 1.21E\left(\frac{t}{r}\right)^2$$

$$\nu = 0.2 \qquad q_{cr} = 1.18E\left(\frac{t}{r}\right)^2$$

and also for

$$\nu = 0 \qquad q_{cr} = 1.16E\left(\frac{t}{r}\right)^2$$

Von Kármán and Tsien in 1939 published the results of their non-linear studies and came to a value of $0.36E(t/r)^2$. By refining the theory Tsien found (1942) a coefficient of 0.312; Muschlari (1950): 0.34 and Feodosjew (1954): 0.32.

Ebner [4] published (in 1962) a comprehensive review of the maximum and minimum values of q_{cr}. It is done for complete spheres having different radii and thicknesses; results from various theories as well as experimental researches were given. The values

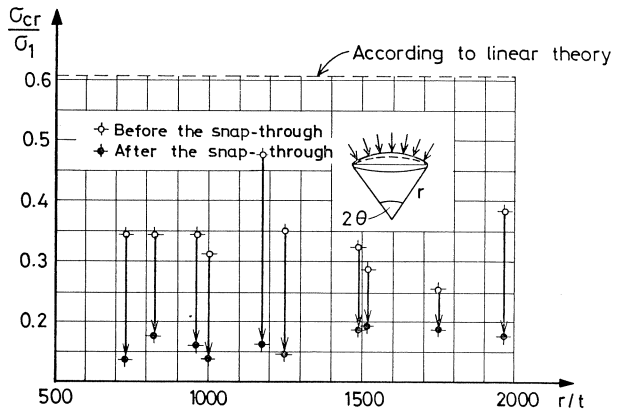

Fig. 6.
Max. and min. values of buckling stresses for spheres under external pressure, reported by Wolmir.

run from $1.16E(t/r)^2$ as a maximum to $0.16E(t/r)^2$ as a minimum; this resulting from upper bound and lower bound theories as well as from experimental data. Wolmir [5] reports on metal domes having an angle of aperture θ of $\sim 18°$ and thicknesses of 0.34 resp. 0.45 mm (fig. 6).

It is evident that the results cannot serve as a base for practical design and calculations of the buckling. For the doubly curved shells in general the situation is no better. Nevertheless they are increasingly used.

Csonka suggested a formula employing the product of the principal radii of curvature:

$$q_{cr} = \alpha E \frac{t^2}{r_1 r_2}$$

and the problem was to determine or to know the value of α. Experimental work by Mehmel [6] and by Schmidt [7] lead to varying values. Schmidt tested eight aluminium translation shells and arrived at an average value of $\alpha = 0.32$; he varied the two principal radii relation r_x/r_y from 10/3 to 5/3. For a spherical shell made of plexiglass bearing on six supports Mehmel found a value of $C = \alpha = 0.52$. A summary of the values af α, listed by Schmidt, was again published in 1967 [9].

If comparison is made to the mentioned value of 1.16 for a dome, one should be aware that here we deal with parts of a shell surface, against the full dome mentioned before.

Moreover it should be clear that the application of the mentioned formula of $q_{cr} = \alpha E(t^2/r_1 r_2)$ certainly has its limits. It has the disadvantage of predicting a zero buckling load when one of the curvatures $(1/r)$ becomes zero.

II Stability of doubly curved shells having a positive curvature index

Buckling of a spherical dome

For the calculation of the buckling load the energy stored in the area of the snap-through will be determined as a function of the diameter and the rise. Buckling will occur when the difference between the internal energy and the work performed by the external forces becomes a minimum.

For the non-linear part of the spherical dome a new buckling shape has been chosen.

It will be axial-symmetrical and its formula is:

$$w_1 = f\left\{1 - \left(\frac{r}{c}\right)^2\right\} + \frac{qR^2}{2Et}; \tag{1}$$

w is the radial deformation in the snap-through area (fig. 7). f denotes the rise and c the radius of the snap-through area.

The term $qR^2/2Et$ represents the membrane deflection due to the unit load q; R being the radius of the dome.

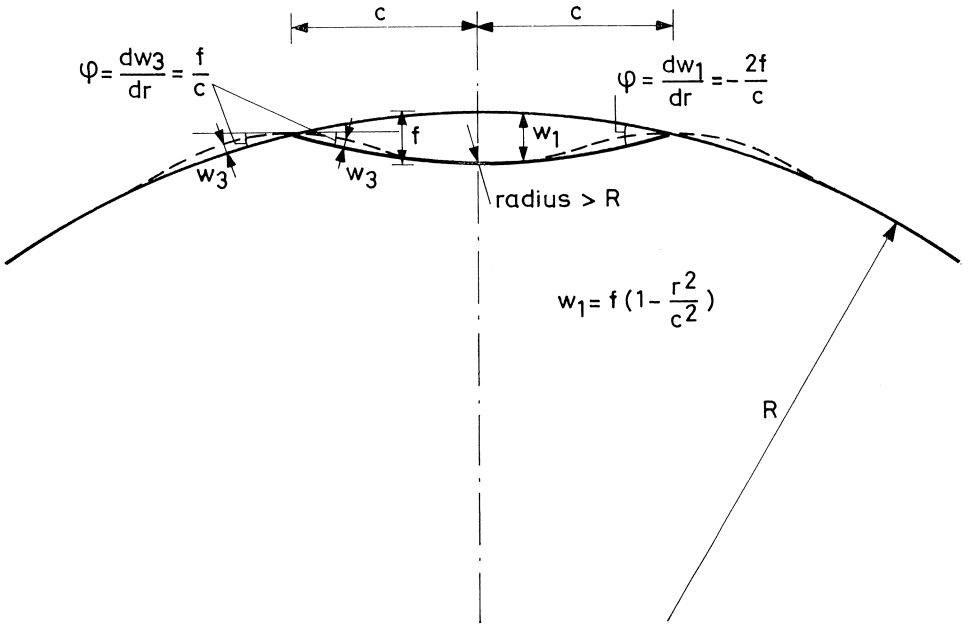

Fig. 7. Deflection of the snap-through-area.

On the pattern of deformation an edge disturbance has been superimposed so that a uniform and continuous angular deformation dw/dr will occur. This angular rotation has been calculated by means of the Geckeler's approximation and we write:

$$w_2 = -\frac{f}{c\lambda} e^{+\lambda(r-c)} \sin \lambda(r-c) \tag{2}$$

Accordingly the total deformation of the snap-through area will be:

$$w_1 + w_2 = f\left\{1 - \left(\frac{r}{c}\right)^2\right\} + \frac{qR^2}{2Et} - \frac{f}{\lambda} e^{\lambda(r-c)} \sin \lambda(r-c); \tag{3}$$

and for the remainder part of the sphere:

$$w_3 = -\frac{f}{c\lambda} e^{+\lambda(c-r)} \sin \lambda(c-r) + \frac{qR^2}{2Et} \tag{4}$$

A stress-function is chosen and the stresses (σ_r and σ_φ) can be calculated, including the application of the boundary conditions.

The internal energy performed by the membrane stress will be defined by

$$U_m = \frac{t}{2E} \int_0^c (\sigma_r^2 + \sigma_\varphi^2) 2\pi r \mathrm{d}r \tag{5}$$

The internal energy performed by bending in the snap-through area amounts to

$$U_b = \frac{Et}{2}\int_0^c \left\{\left(\frac{1}{r}\frac{dw}{dr}\right)^2 + \left(\frac{d^2w}{dr^2}\right)^2\right\} 2\pi r dr \tag{6}$$

The energy due to the load q during the snap-through (which may be called external energy) is:

$$U_q = \int_0^c q\left(w_1 - \frac{qR^2}{4Et} + w_2\right) 2\pi r dr \tag{7}$$

Thus the energy to be observed will be: $U = U_m + U_b - U_q$.

From the application of the two minimum criteria:

$$\frac{\partial U}{\partial f} = 0 \quad \text{and} \quad \frac{\partial U}{\partial c} = 0$$

follow two equations from which q as a function of f and as a function of c can be determined.

This calculation has to be done numerically. The result was a minimum value of q for $f = 16t$. Then the critical value of q can be expressed to be:

$$q_{cr} = 0.34\frac{Et^2}{R^2}$$

This value coincides rather well with the value derived by Von Kármán and Tsien [8].

The function of w used by them and the boundary condition of the snap-through area differ from the assumption made by the authors. A similar difference exists with the derivation given by Wolmir [5].

One should be aware of the fact that all the studies were confined to axial symmetry; in regard to the shell and also in reference to the assumed buckling pattern. As a next step an elliptic surface was considered; for the shell as well for the snap-through area.

The elliptic surface

For the deflection in the snap-through area is assumed the equation: (fig. 8)

$$w_1 = f\left(1 - \frac{x^2}{a_1^2} - \frac{y^2}{b_1^2}\right) \tag{8}$$

Again the assumption is made that the edge of this area is located in a flat plane.

The solution (w_1, φ_1) together with the particular solution (w_2, φ_2) including the edge disturbance (w_3, φ_3) must satisfy the equation

$$-\frac{Et^2}{12}\Delta\Delta w + \frac{1}{R_1}\frac{\partial^2 \Phi}{\partial y^2} + \frac{1}{R_2}\frac{\partial^2 \Phi}{\partial x^2} + \frac{q}{t} = 0$$

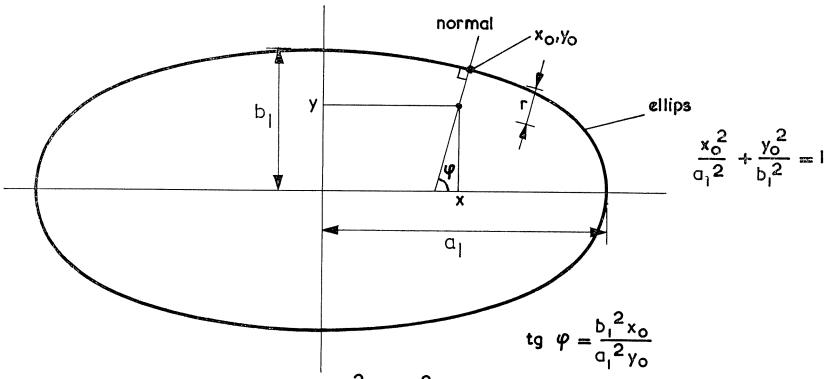

$$x = x_o - \frac{r x_o}{a_1^2} x_o^{-1/2}$$

$$y = y_o - \frac{r y_o}{b_1^2} x_o^{-1/2}$$

Fig. 8. The snap-through area an elliptic surface; transformation of coördinates.

The stress-function Φ_1 derived for the deflection w_1, is determined by the equation:

$$\frac{1}{E} \Delta\Delta\Phi_1 + \left\{ \left(\frac{\partial^2 w_1}{\partial x \partial y} \right)^2 - \frac{\partial^2 w_1}{\partial x^2} \cdot \frac{\partial^2 w_1}{\partial y^2} \right\} + \frac{1}{R_1} \frac{\partial^2 w_1}{\partial y^2} + \frac{1}{R_2} \frac{\partial^2 w_1}{\partial x^2} = 0$$

As a boundary condition to Φ_1 it is assumed that the deformations in the tangential directions u and v are zero at the edge of the snap-through area.

For the boundary conditions of w again two requirements are needed. First $w=0$ for the circumference; secondly the first derivaties $\partial w/\partial x$ and $\partial w/\partial y$, the angular rotations should be continuous and similar (fig. 9).

For the membrane state of stresses the equation

$$\frac{N_x}{R_1} + \frac{N_y}{R_2} + q = 0$$

governs the problem. If the load is divided in two parts, we can define:

$$\frac{N_y}{R_2} = -\alpha q \quad \text{and} \quad \frac{N_x}{R_1} = -(1-\alpha) q$$

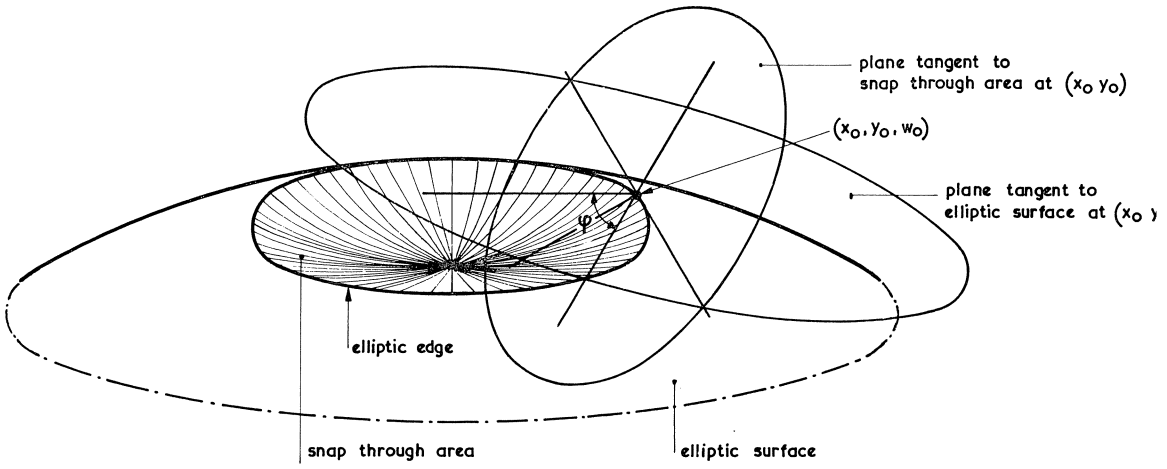

Fig. 9.

For a dome ($R_1 = R_2$) having an uniform load q, the value of α will be $\alpha = 0.5$. In the case of an arch with $R_1 = \infty : \alpha = +1$, and with $R_2 = \infty$, $\alpha = 0$.

The deflection of the membrane is calculated by determining the energy performed by the load and by the membrane forces, both in the snap-through area:

$$\tfrac{1}{2}\int_A w_2 q \mathrm{d}A = \frac{1}{2Et}\int_A (N_x^2 + N_y^2)\mathrm{d}A = \frac{1}{2Et}\int_A \{R_1^2(1-\alpha)^2 q^2 + R_2^2\alpha^2 q^2)\mathrm{d}A\}$$

$$\text{or} \quad w_2 = \frac{q}{Et}\{R_1^2(1-\alpha)^2 + R_2^2\alpha^2\} \tag{9}$$

This under the assumption that the membrane forces do not vary in the snap-through area (indicated as A).

In order to determine the angular rotation at the edge of this area the tangent plane to $w_1 = f(1-x^2/a_1^2 - y^2/b_1^2)$ should be formulated. In a point $(x_0 y_0 z_0)$ of the elliptic edge it will be, (figs. 8 and 9)

$$\frac{2fx_0}{a_1^2}(x-x_0) + \frac{2fy_0}{b_1^2}(y-y_0) + w - w_0 = 0$$

The vertical plane through the normal in the point $(x_0 y_0)$ of ellips is:

$$\frac{a_1^2 y_0}{b_1^2 x_0}(x-x_0) - (y-y_0) = 0$$

Next the intersecting lines l_1 and l_2 of the tangent plane respectively the horizontal

plane through the described normal can be determined by formulating the direction-coefficients, and the angle between these two lines can be derived:

$$\varphi \sim \operatorname{tg}\varphi = 2f\left(\frac{x_0^2}{a_1^4} + \frac{y_0^2}{b_1^4}\right)^{\frac{1}{2}}$$

The boundary disturbance extends at two sides viz. along the inside as well along the outside of the snap-through area. For both regions again the assumption is made that its course will be according to the approximation of Geckeler:

$$w_3 = Ae^{-\lambda r}\sin\lambda r \quad \text{with} \quad \lambda = \frac{\sqrt[4]{3}}{\sqrt{Rt}} \tag{10}$$

inserting for R the radius of curvature along the normal in the point $(x_0 y_0)$.

For the further elaboration one is referred to the publication [10] where every step has been shown. The expressions for w_1, w_2 and w_3 have been formulated and will be substituted one by one in the comptability equation.

Also the shell forces belonging to the edge disturbance and acting in the direction perpendicular to the normal as well as in the direction of the normal can be determined. From them the shell forces in the x- en y-direction can be formulated: N_x, N_y and N_{xy}. When the deflections and the normal forces in the snap-through area are determined, the energy due to the normal forces (U_m), to the bending moments (U_b) and to the load (U_q) can be formulated. Then the minimum criteria will be applied to the expression $U = U_n + U_b - U_q$ and the snap-through load together with the size buckling area can be determined. Omitting the influence of the contraction ($v = 0$) the expressions are:

$$U_n = \frac{1}{2Et}\int_A (N_x^2 + N_y^2 + 2N_{xy}^2)\mathrm{d}A$$

$$U_b = \frac{Et}{2}\int_A \left\{\left(\frac{\partial^2 w}{\partial x^2}\right)^2 + \left(\frac{\partial^2 w}{\partial y^2}\right)^2 + 2\left(\frac{\partial^2 w}{\partial x \partial y}\right)\right\}\mathrm{d}A$$

$$U_q = \int_A q(w_1 + \tfrac{1}{2}w_2 + w_3)\,\mathrm{d}A$$

To facilitate the calculations the following substitutions are introduced in order to determine the minima $\partial U/\partial f$ and $\partial U/\partial c$.

$$f = \varphi t, \quad c = \Psi\sqrt{R_2 t}, \quad q = \gamma\frac{Et^2}{R_2^2}$$

$$\frac{\partial U}{\partial f} : \gamma\left(\varphi - \frac{\sqrt{3}}{3}\right) = \frac{7}{12}\frac{\varphi}{\Psi^2}(2\varphi^2 - 3\varphi\Psi^2 + \Psi^4) + \frac{q}{80\sqrt[4]{3}} + \frac{\varphi^3}{\Psi^3} +$$

$$\frac{2\sqrt[4]{3}}{3}\frac{\varphi}{\Psi} + \frac{\varphi}{2\Psi^4}(\Psi\sqrt[4]{3} - \tfrac{3}{2})(3\varphi - 2\Psi^2) \quad \text{and}$$

$$\frac{\partial U}{\partial c} = \varphi^2\left(\frac{7}{12}\Psi^2 + \frac{27}{320\sqrt[4]{3}}\Psi + \varphi\left(\frac{3\Psi\sqrt[4]{3}}{2} - 3\right) - \frac{7\Psi^6}{12} - \frac{\Psi^3\sqrt[4]{3}}{6} + \frac{3\Psi^2}{2}\right) = 0$$

From the latter expression for each value of ψ, φ can be calculated. Substitution in the other equation gives the value of γ. In fig. 10 the results of these calculations are shown for three cases.

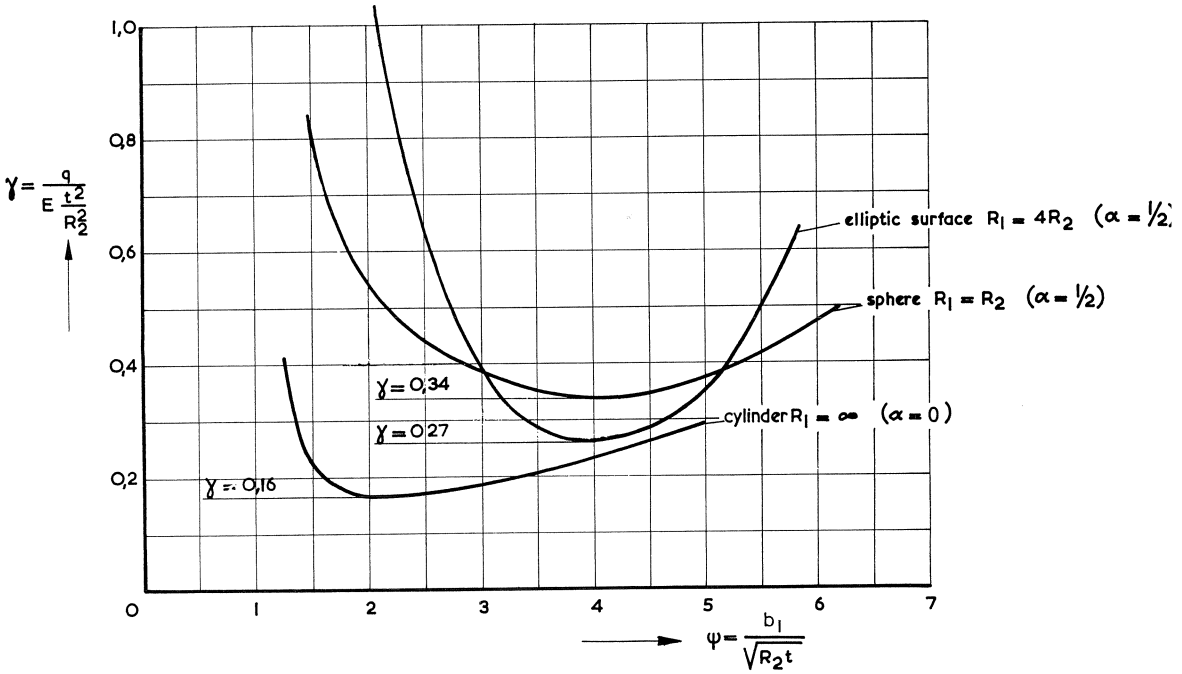

Fig. 10. Buckling load as function of a signifigant dimension of the snap-through-area.

Specific cases

Related to shape there are two extrema, the spherical shell and the cylindrical shell. The latter can also be taken as an arch.

For the sphere we write:

$$a_1 = b_1 = c; \quad R_1 = R_2 = R; \quad A = \tfrac{1}{8}; \quad x_0^2 + y_0^2 = R^2 \quad \text{and} \quad \alpha = 0.5$$

Again the expression for $U = U_n + U_b - U_q$ is differentiated in respect to f and c respectively. To facilitate the calculations the following substitions are made:

$$f = \varphi t, \quad c = \Psi\sqrt{Rt}, \quad q = \gamma\frac{Et^2}{R^2}$$

When the minimum criteria are applied ($\partial U/\partial f = 0$, $\partial U/\partial c = 0$) the minimum value appears to be:

$$q_{cr} = 0.34\frac{Et^2}{R^2},$$

a wellknown value. It proves that for $R_1 = R_2$ the buckling load is in dependent of α.

For the cylindrical shell we write:

$$a_1 = \infty,\ b_1 = 0,\ y_0 = \pm c,\ R_1 = \infty,\ R_2 = R \text{ and } \alpha = 0.$$

When beforehand the expression for U has been divided by a_1, it becomes:

$$U = \frac{5\pi}{9}\frac{Etf^2}{c^3}\left(f - \frac{c^2}{R}\right)^2 + \frac{q}{160\sqrt[4]{3}}\frac{Et^{3/2}f^4R^{1/2}}{c^4} + \frac{Et^{5/2}f^2}{2.3^{3/4}c^2R^{1/2}} - \frac{\pi qf^2R}{2c} +$$
$$+ \frac{2Et^3f^2}{3c^3} + \frac{4}{3^{1/2}}\frac{qftR}{c}$$

Introducing the mentioned substitutions the minima will be:

$$\frac{\partial U}{\partial f} = 0;\ \gamma\left(\pi\varphi - \frac{4\sqrt{3}}{3}\right) = \frac{10\pi}{9}\frac{\varphi}{\Psi^2}(\varphi - \Psi^2)(2\varphi - \Psi^2) + \frac{\varphi}{3^{3/2}\Psi} + \frac{4}{3}\frac{\varphi}{\Psi^2} + \frac{9\varphi^3}{40\sqrt[4]{3}\cdot\Psi^3}$$

$$\frac{\partial U}{\partial c} = 0;\ \gamma\left(\pi\varphi - \frac{8\sqrt{3}}{3}\right) = \frac{10\pi}{9}\frac{\varphi}{\Psi^2}(\varphi - \Psi^2)(3\varphi + \Psi^2) + \frac{2\varphi}{3^{3/4}\Psi} + \frac{4\varphi}{\Psi^2} - \frac{27\varphi^4}{160\sqrt[4]{3}\cdot\Psi^4}$$

The minimum value appears to be:

$$q_{cr} = 0.16\frac{Et^2}{R^2}$$

When considered as a linear load, and for a cylinder:

$$q_{cr} = \sigma_{cr}\frac{t}{R}: \quad \sigma_{cr} = 0.16E\frac{t}{R}$$

Pogorelov [11] in his book on the geometrical methods of non-linear theories of shells (Moscow 1967) gives a value of $\sigma_{cr} = 0.16Et/R$ for a cylindrical shell having a relation $R/t = 500-1300$.

For an *elliptic surface* having

$$R_1 = 4R_2, \quad a_1 = 2b_1 \quad \text{and} \quad \frac{x_0^2}{4} + y_0^2 = b^2$$

the expression for the total energy U and the two derivatives leading to the minima can be written down. They are long expressions with many terms. In addition we have introduced $\alpha = \frac{1}{2}$ which means that an equal division of the load is assumed in both directions (x and y). Then follows a critical load:

$$q_{cr} = 0.27 \frac{Et^2}{R_2^2}$$

In addition calculations have been executed for $\alpha = 0$ and $\alpha = 1$. They are shown as a function of q_{cr} (fig. 11). It appears that the choice of α has a small influence on the magnitude of the critical load (fig. 12); it varies from $q_{cr} = 0.25$ to $0.29Et^2/R_2{}^2$.

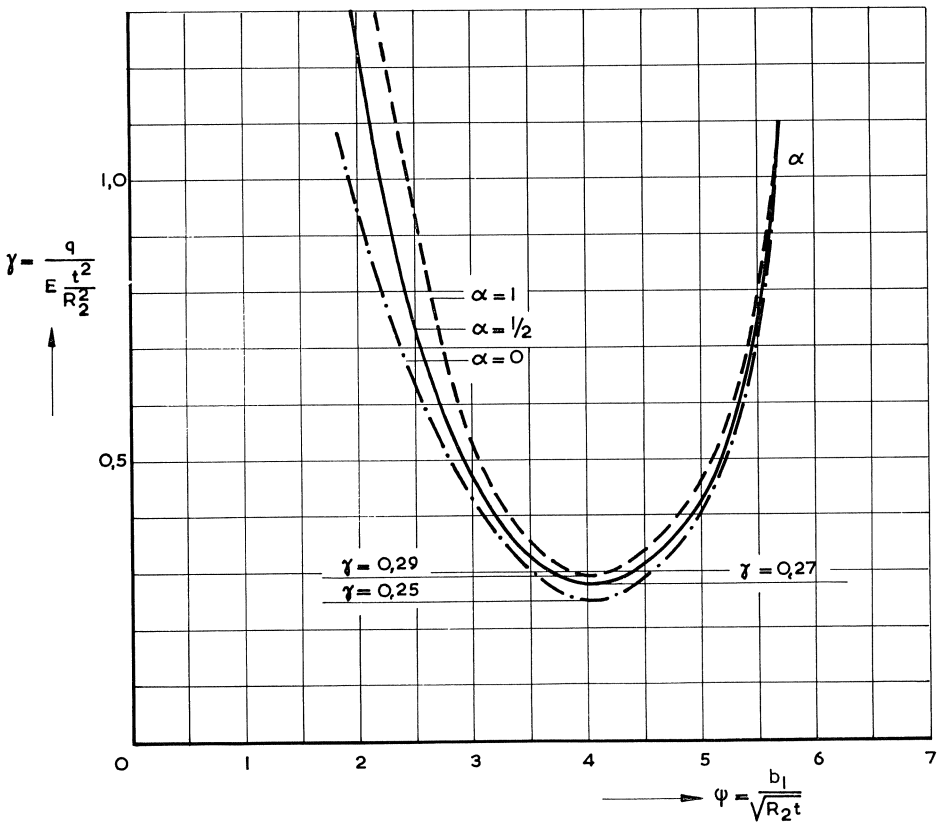

Fig. 11. Buckling load of the elliptic surface $R_1 = 4R_2$ for different values of α.

In fig. 10 the minima of the coefficient $\gamma = q/(Et^2/R_2{}^2)$ are plotted as function of $\psi = b/\sqrt{R_2 t}$ representing a dimensionless function of a significant dimension of the observed snap-through area. Thus combined in one figure are given the $\gamma_{\min}$ for the cylinder ($R_1 = \infty$, $\alpha = 0$), the sphere ($R_1 = R_2$, $\alpha = \frac{1}{2}$) and the elliptic surface ($R_1 = 4R_2$, $\alpha = \frac{1}{2}$), and in this sequence they amount to: $\gamma = 0.16$; 0.34 and 0.27.

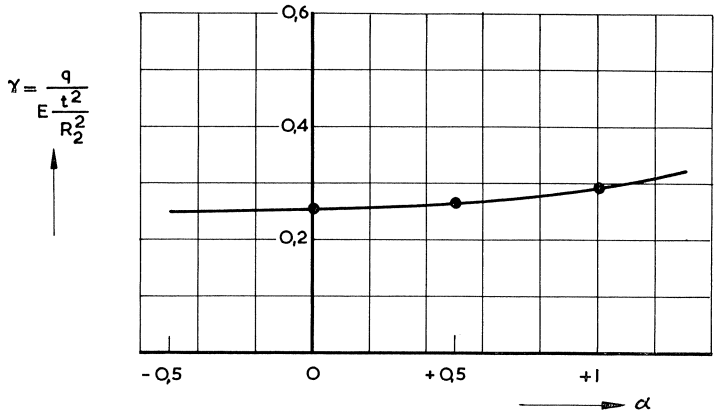

Fig. 12. The influence of the parameter α on the buckling load.

In figure 13 these minima are given as a function of R_2/R_1. Thus for $R_2/R_1 = 0$ it represents the cylinder with a radius R_2; and for $R_2/R_1 = 1$ it is the sphere. Between these two extremes the values of the elliptic surface will be found. For $R_2/R_1 = 0.25$ the calculated value equals $\gamma = 0.27$. These three values are located on the curve 1.

It should be noted that the assumptions are $R_2 < R_1$ and also both radii to be positive. The observed range extends from $R_2/R_1 = 0$ to $R_2/R_1 = 1$; the areas outside of it viz $R_2/R_1 < 0$ and $R_2/R_1 > 1$ are not included. It means that at this stage hyperbolic paraboid shells are omitted from the stability considerations.

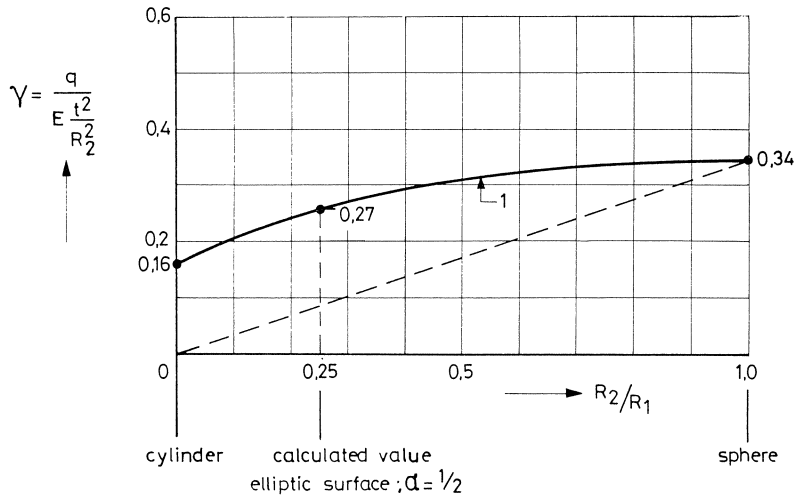

Fig. 13. Buckling load as function of R_2/R_1.

The coefficient γ for $R_2/R_1 = 1$, the sphere, is known and has already determined by others e.g. by Von Kármán and Tsien.

The criterion $R_2/R_1 = 0$ may lead to the conception of the circular cylinder as well as to the arch. It depends whether the x- or y-direction is observed (fig. 14). As has announced in the foreword a further publication will deal with these extrema at large as well as with the extension in the area of the doubly curved shells having a negative curvature index.

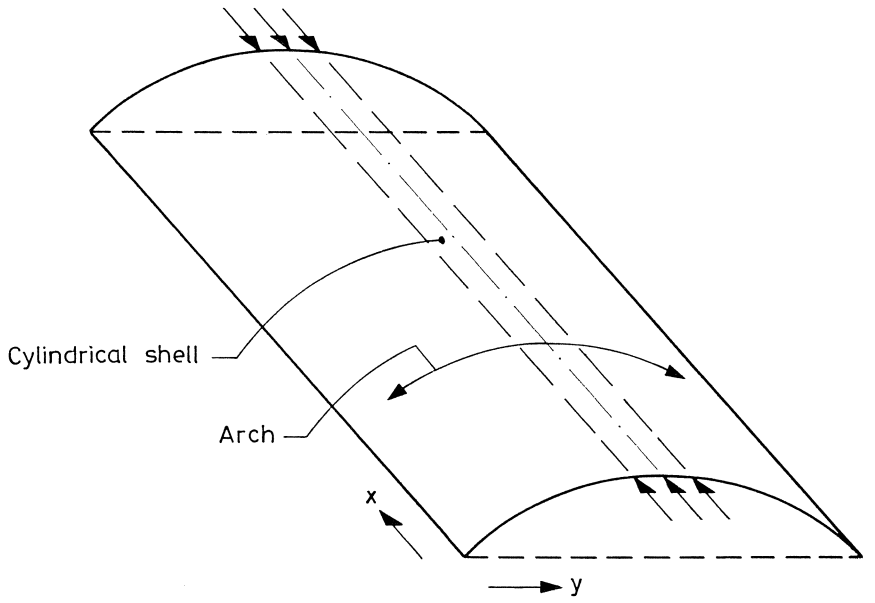

Fig. 14.

In concluding the authors like to point out that the method of calculation exposed in this chapter proves to be very flexible in regard to the introduction or deletion of terms. If for the sake of refinement of the results modifications or new terms are to be included the result of them can be followed closely. Likewise when a term is deleted the result can be traced clearly.

III The influence of the edge stiffness and of the angle of aperture

It may be well to reflect on the procedure followed so far. The load – deflection – curve has a linear and a non-linear-part (fig. 15). For the buckled form a paraboloid of revolution was chosen. A reasonable assumption is that the segment under consideration will be bounded by a flat plane ($r = c$). The buckled form will push through it and as a result the post-buckling form will mirror itself in reference to this plane. Strains in the membrane are neglected. Furthermore a boundary disturbance at the

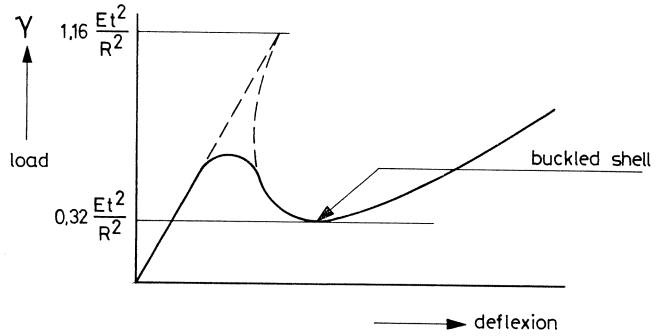

Fig. 15.

circumference of the snap-through area is assumed, introduced as an angular rotation, being equal and continuous along the circular edge.

Von Kármán and Tsien assumed a different buckled form based on the deflections of a circular plate restrained as the boundary. This assures a continuous course of buckling shape (without knicks) unto the undisturbed part of the shell. However it leads to a stress distribution in which there are discontinuities. Wolmir in his publication has chosen a similar form:

$$w = f\left(1 - \frac{r^2}{c^2}\right)^2$$

For a complete sphere this rigid requirement for the edge of the snap-through-area may be acceptable. However for a segment of a sphere it will not be possible to satisfy this requirement.

In the following part an attempt is made to determine the influence of a partial restraint along the edge of the considered segment. In order to cope with it the shape of the snap-through-area has been built up of two parts: one part connected with a knick to the remainder part of the shell: a discontinuity. Its shape corresponds to the mirrored part of the shell segment. The other part is limited to the edge of the snap-through-area and may be considered as an edge-disturbance-area. This splitting-up makes it possible to result in a continuous connection with the edge-beam: a realistic assumption as compared to the classical one (fig. 16). The rise (f) and diameter ($2c$)

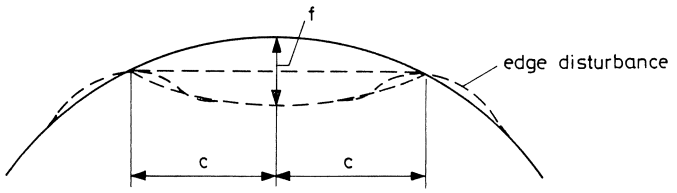

Fig. 16.

of the buckled area are kept variable. Then the values of these variables for which the load is a minimum are determined. This approach of the buckled form enables us to follow the pattern of the snap-through phenomena as it develops.

The snap-through begins in a very small area. It will start from a small discrepancy in the original shape of the sphere. This post-buckled shape will equal the original shape and will be mirrored in regard to the flat plane through the circumference of the buckled area (fig. 17). In this small area there will hardly be normal (membrane-) forces. However, for this state of shell-stresses the energy of the internal forces does not equal the energy exerted by the external forces and therefore the buckled area will increase and the load on the shell proper, depending on the loading system, decreases.

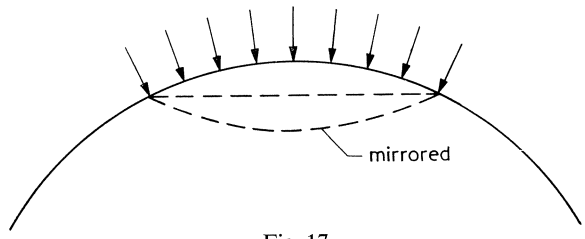

Fig. 17.

Due to the increment of the buckled area the angle of aperture increases and the angular rotation along the edge as well. This rotation along the edge has to be resisted by an edge disturbance.

Apparently the part of the energy of the internal forces generated by the edge disturbance will augment quicker when the buckled area increases. Finally, when the "internal" energy equals the "external" one a state of equilibrium is reached and the snap-through phenomenon will become stable. A rough approximation may clarify this procedure.

The energy caused by the load on the buckled area is about $U_q = qfc^2$. Due to the buckled form $f \approx c^2/R$ and therefore:

$$U_q = \frac{1}{R} qc^4$$

In accordance with the preceding, the "internal" energy should increase more rapidly than the "external" one, when c becomes larger. Thus the energy of the internal forces must increase swifter than c^4.

From what has been stated in regard to the mirrored form of buckling phenomenon, the energy of the normal forces in the buckled area can be neglected. The work done by the bending moments caused by a constant curvature of the buckled area is proportional to c^2.

Enlargement of the snap-through area can only be prevented by an increase of the energy due to the edge disturbance. The angle of rotation of the edge is about $f/c \approx c/R$.

At a distance of the edge of $1/\lambda = \sqrt[4]{Rt}/\sqrt[4]{3}$ the deflection equals $w = c/R\lambda$. Therefore the stress σ_φ will be $\sigma_\varphi = Ew/R = Ec/\lambda R^2$; all according to the Geckeler approximation. In terms of energy we write

$$\frac{\partial U}{\partial V} = \tfrac{1}{2}\frac{\sigma^2}{E} = \frac{1}{2E}\left(\frac{Ec}{\lambda R^2}\right)^2 = \frac{E}{2}\left(\frac{c}{\lambda R^2}\right)^2$$

The total internal energy generated for the whole area will be

$$U = \frac{t}{2E}\int_0^c (\sigma_r^2 + \sigma_\varphi^2)2\pi r \mathrm{d}r$$

For $\sigma_r = 0$, the expression leads to:

$$U = 2\pi ct\frac{E}{2}\left(\frac{c}{\lambda R^2}\right)^2 = \pi cEt\left(\frac{c}{\lambda R^2}\right)^2$$

and will be proportional to c^3.

The part of the energy equation which can call a halt to a further spreading comes from the non-linear part. The strain of the surface can be expressed as:

$$N_r = \tfrac{1}{2}Et\left(\frac{\mathrm{d}w}{\mathrm{d}r}\right)^2$$

Because of the large deflection can be written:

$$\frac{\mathrm{d}w}{\mathrm{d}r} \approx \lambda w,$$

and then

$$N_r \approx \tfrac{1}{2}Et\lambda^2 w^2 = \frac{Et\lambda^2 c^2}{2R^2\lambda^2} = \frac{Etc^2}{2R^2} = \frac{Et}{2}\,\frac{c^2}{R^2}$$

The total energy along the edge will be

$$U \approx \frac{Et}{8}\left(\frac{c^2}{R^2}\right)^2 2\pi c$$

and thus is proportional to c^5.

Apparently, this non-linear part of the edge disturbance is the only part that can stop the spreading of the snap-through for sufficient large values of c.

Thus it appears to be important to determine these terms more accurate. However this will lead to rather complicated mathematical analyses that only can be solved by means of numerical calculations.

In this approach an approximation is used; a more accurate calculation may be developed later. The impression is that this will result in somewhat larger snap-through areas.

The snap-through area will mostly start along an edge or an opening because in many cases the edge-beam will not have sufficient stiffness to prevent rotation and thus will not present the same energy as can be supplied by the remaining part of the shell, where it is continuous. Specially in those cases where the edge-beam occupies an important part of the edge of the snap-through area the relative stiffness of the edge-beam will be of importance (fig. 18).

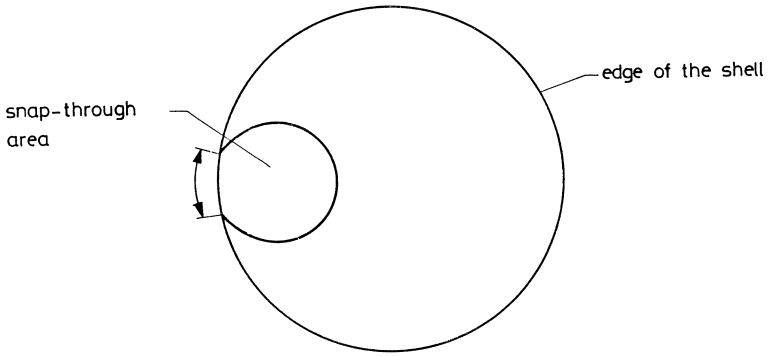

Fig. 18.

Resuming the critical load will be dependent on:

a. The measure of coincidence of the snap-through edge and the edge-beam.
b. The relative stiffness of the edge-beam.

In the next part of influence the angle of aperture and of the edge-beam stiffness on the critical load will be investigated for a part of a sphere.

First the calculation as developed for a spherical shell will be restated and later adapted to the introduction of an edge-beam.

The radial deformation of the snap-through area has been expressed:

1. Due to the membrane action:

$$w_1 = \frac{qR^2}{2Et} \tag{1}$$

2. Due to the snap-through phenomenon:

$$w_2 = f\left\{\left(1 - \frac{r}{c}\right)^2\right\} \tag{2}$$

3. Due to the edge disturbance:

$$w_3 = Be^{-\lambda(c-r)} \sin \lambda (c-r) \quad \text{for} \quad (r \leqq c) \tag{3}$$

thereby introducing a parameter $B = f/c\lambda$.

If $r = c$ then is $w_2 = w_3 = 0$.

The parameter λ is similar to the one used in the approximation by Geckeler:

$$\lambda = \frac{\sqrt[4]{3}}{\sqrt{Rt}} \tag{4}$$

For the sequence mentioned the angular rotation dw/dr at the edge $r = c$ is:

$$\begin{aligned} \left(\frac{dw_1}{dr}\right)_c &= 0 \\ \left(\frac{dw_2}{dr}\right)_c &= \frac{-2f}{c} \\ \left(\frac{dw_3}{dr}\right)_c &= -\lambda B \end{aligned} \tag{5}$$

The normal stresses shall now be determined using the equation of compatibility for large deformations:

$$\frac{d}{dr}\left\{\frac{1}{r}\frac{d}{dr}\left(r\frac{d\Phi}{dr}\right)\right\} = -E\left\{\frac{1}{2r}\left(\frac{dw}{dr}\right)^2 + \frac{1}{R}\frac{dw}{dr}\right\} \tag{6}$$

in which Φ is a stress function: $\sigma_\varphi = d^2\Phi/dr^2$.

Substitution of w_1 leads to the known expressions:

$$\sigma_{r_1} = \frac{-qR}{2t} \quad \text{and} \quad \sigma_{\varphi_1} = -\frac{qR}{2t} \tag{7}$$

Substitution of the formula for w_2 gives:

$$\Phi_2 = -\frac{Ef}{16c^2} r^4 \left(\frac{f}{c^2} - \frac{1}{R}\right) + \frac{A_1 r^2}{4} - A_2 \ln r + A_3 \tag{8}$$

A_3 is an arbitrary constant.

The constants A_1 and A_2 can be determined from the boundary conditions:

$$\begin{aligned} r = c \qquad & \sigma_\varphi = 0 \\ r = 0 \qquad & \sigma_\varphi \neq \infty \end{aligned}$$

Then the stresses will be:

$$\sigma_{r_2} = -\frac{Ef}{4}\left(\frac{f}{c^2}-\frac{1}{R}\right)\left(\frac{r^2}{c^2}-3\right)$$

$$\sigma_{\varphi_2} = -\frac{3Ef}{4}\left(\frac{f}{c^2}-\frac{1}{R}\right)\left(\frac{r^2}{c^2}-1\right) \tag{9}$$

For the mirrored form $f = c^2/R$, $\sigma_{r_2} = \sigma_{\varphi_2} = 0$.

Introducing the formula for w_3 in the equation:

$$\frac{\mathrm{d}}{\mathrm{d}r}\left\{\frac{1}{r}\frac{\mathrm{d}}{\mathrm{d}r}\left(r\frac{\mathrm{d}\Phi}{\mathrm{d}r}\right)\right\} = -E\left\{\frac{1}{2r}\left(\frac{\mathrm{d}w}{\mathrm{d}r}\right)^2+\frac{1}{R}\frac{\mathrm{d}w}{\mathrm{d}r}\right\}$$

which can be written as:

$$\frac{\mathrm{d}}{\mathrm{d}r}\left\{\frac{1}{r}\frac{\mathrm{d}\Phi}{\mathrm{d}r}+\frac{\mathrm{d}^2\Phi}{\mathrm{d}r^2}\right\} = -E\left\{\frac{1}{2r}\left(\frac{\mathrm{d}w}{\mathrm{d}r}\right)^2+\frac{1}{R}\frac{\mathrm{d}w}{\mathrm{d}r}\right\}$$

or as:

$$\frac{\mathrm{d}}{\mathrm{d}r}(\sigma_\varphi+\sigma_r) = -E\left\{\frac{1}{2r}\left(\frac{\mathrm{d}w}{\mathrm{d}r}\right)^2+\frac{1}{R}\frac{\mathrm{d}w}{\mathrm{d}r}\right\}$$

does not lead to a solution in a closed formula. Integrals of the type

$$\int_0^c \frac{e^{-\lambda(c-r)}}{r}\sin\lambda(c-r)\,\mathrm{d}r$$

occur. These integrals can only be determined numerically.

An approximate solution of the equation of compatibility can be written introducing the parameter A:

$$\sigma_{\varphi_3} = \frac{\mathrm{d}^2\Phi}{\mathrm{d}r^2} = EA\left(\frac{\lambda A r}{2c^2}-\frac{1}{R}\right)e^{-\lambda(c-r)}\sin\lambda(c-r)$$

$$\sigma_{r_3} = \frac{1}{r}\frac{\mathrm{d}\Phi}{\mathrm{d}r}-\frac{E}{2}\left(\frac{\mathrm{d}w}{\mathrm{d}r}\right)^2 =$$

$$= \frac{EA}{2\lambda c}\left(\frac{\lambda A r}{2c^2}-\frac{1}{R}\right)e^{-\lambda(c-r)}\{\sin\lambda(c-r)-\cos\lambda(c-r)\}^2+$$

$$-\frac{E}{2}(\lambda B)^2 e^{-2\lambda(c-r)}\{\sin\lambda(c-r)-\cos\lambda(c-r)\}^2 \tag{10}$$

The first term in the expression for σ_{r_3} is rather small compared with the second one and is neglected in the following computations.

If A = 0 then $\sigma_{\varphi_3} = 0$ (no edge disturbance).

If $r = c$, $\sigma_{\varphi_3} = \sigma_{r_3} = 0$ in the case that:

$$\left(\frac{\lambda A r}{2c^2} - \frac{1}{R}\right) = 0$$

Then

$$A = \frac{2c^2}{\lambda R r} = \frac{2c}{\lambda R} \quad (r = c)$$

This may be described as an edge disturbance without having membrane stresses at the edge. In this case the angular rotation along the edge of the snap-through area is zero. Thus the edge will be completely restraint. The angular rotation is calculated from:

$$\frac{d}{dr}\left\{\frac{1}{R}\frac{d}{dr}\left(r\frac{d\Phi}{dr}\right)\right\}_{r=c} = -E\left\{\frac{1}{2r}\left(\frac{dw}{dr}\right)^2 + \frac{1}{R}\frac{dw}{dr}\right\}_{r=c}$$

Substitution of $\sigma_{\varphi_3} = d^2\Phi/dr^2$ leads to:

$$\frac{EA}{2}\left\{\frac{1}{c^2 R} - 2\lambda^2\left(\frac{\lambda A}{2c} - \frac{1}{R}\right) + \frac{A}{2c^2}\left(\frac{1}{c^2} - \frac{\lambda}{c}\right)\right\} = -E\left\{\frac{1}{2r}\left(\frac{dw}{dr}\right)^2 + \frac{1}{R}\frac{dw}{dr}\right\}_{r=c}$$

This can be approximated to:

$$-EA\lambda\left(\frac{\lambda A}{2c} - \frac{1}{R}\right) = -E\left\{\frac{1}{2c}\left(\frac{dw}{dr}\right)_c^2 + \frac{1}{R}\left(\frac{dw}{dr}\right)_c\right\}$$

Introducing for A the expression $\alpha_1(c/\lambda R)$ it will be possible to have a stiffness coefficient fluctuating from $0 \leqq \alpha_1 \leqq 2$, viz. from free to very rigid.

For

$$A = \alpha_1 \frac{c}{\lambda R} \tag{11}$$

The result is:

$$\left(\frac{dw}{dr}\right)_{r=c} = \frac{c}{R}\left\{-1 \pm \sqrt{1 + 2\alpha_1\left(\frac{\alpha_1}{2} - 1\right)}\right\} = \frac{c}{R}\{-1 \pm (\alpha_1 - 1)\}$$

The two roots are: $-{}_1\alpha(c/R)$ and $(\alpha_1 - r)c/R$.

For $0 < \alpha_1 < 2(dw/dr)$ it fluctuates between 0 and $-2c/R$.

From the formula (3) for w_3:

$$w_3 = Be^{-\lambda(c-r)} \sin \lambda(c-r)$$

the angular rotation is

$$\left(\frac{dw_3}{dr}\right)_c = -\lambda B,$$

see eq. (5).

In this case the result is:

$$B = \frac{\alpha_1 c}{\lambda R} = A$$

From this equality could be deducted that A and B only vary with c. However, the angular rotation dw/dr and also B change as f varies.

$$\frac{c}{R} \approx \frac{f}{c} \quad \text{or} \quad f \approx \frac{c^2}{R}$$

Differention shows that

$$\frac{\partial A}{\partial c} = \frac{\alpha_1}{\lambda R} \quad \text{and} \quad \frac{\partial A}{\partial f} = \frac{\alpha_1}{\lambda c} \tag{12}$$

Energy criterion

The energies of the internal and the external forces will be determined. For the normal forces the internal energy amounts to:

$$U_m = \frac{t}{2E} \int_0^c (\sigma_r^2 + \sigma_\varphi^2) 2\pi r \, dr$$

For the three types of radial deformation this integral should be worked out:

Term	Part of U_m
$\sigma_{r_1}^2 + \sigma_{\varphi_1}^2$	$+\frac{\pi}{4} q^2 \frac{R^2 c^2}{Et}$
$\sigma_{r_2}^2 + \sigma_{\varphi_2}^2$	$+\frac{7}{24} \pi E t f^2 c^2 \left(\frac{f}{c^2} - \frac{1}{R}\right)^2$
$\sigma_{r_3}^2 + \sigma_{\varphi_3}^2$	$+\frac{\pi}{8} E A^2 \left\{\frac{1}{4} \frac{A^2}{c^2} (\lambda c - 3) - \frac{A}{R}\left(1 - \frac{2}{\lambda c}\right) + \right.$
	$\left. + \frac{c}{\lambda R^2}\left(1 - \frac{1}{\lambda c}\right)\right\} + \frac{\pi}{4} E t \lambda^4 A^4 \left(\frac{9}{80} \frac{c}{\lambda} - \frac{11}{800\lambda^2}\right)$

$$2\sigma_{r_1}\sigma_{r_2}+2\sigma_{\varphi_1}\sigma_{\varphi_2} \qquad -\frac{\pi}{2}qRc^2f\left(\frac{f}{2}-\frac{1}{R}\right)$$

$$2\sigma_{r_1}\sigma_{r_3}+2\sigma_{\varphi_1}\sigma_{\varphi_3} \qquad -\frac{\pi qR\mathrm{A}}{2}\left\{\mathrm{A}\left(\frac{1}{2}-\frac{1}{\lambda c}\right)-\frac{c}{\lambda R}\left(1-\frac{1}{\lambda c}\right)\right\}$$

$$-\frac{\pi qR\lambda c\mathrm{A}^2}{8}\left(1-\frac{1}{2\lambda c}\right)$$

$$2\sigma_{r_2}\sigma_{r_3}+2\sigma_{\varphi_2}\sigma_{\varphi_3} \qquad -\frac{3\pi}{2}Etf\mathrm{A}\left(\frac{f}{c^2}-\frac{1}{R}\right)\left\{\frac{\mathrm{A}}{2\lambda c}\left(-1+\frac{5}{2\lambda c}\right)+\right.$$

$$\left.+\frac{1}{\lambda^2 R}\left(1-\frac{3}{2\lambda c}\right)\right\}+$$

$$-\frac{\pi}{8}Etf\lambda c\mathrm{A}^2\left(\frac{f}{c^2}-\frac{1}{R}\right)\left(1+\frac{q}{8\lambda^2c^2}\right)$$

The energy due to bending can be determined from:

$$U_b=\frac{Et^3}{24}\int_0^c\left\{\left(\frac{1}{r}\frac{\mathrm{d}w}{\mathrm{d}r}\right)^2+\left(\frac{\mathrm{d}^2w}{\mathrm{d}r^2}\right)^2\right\}2\pi r\,\mathrm{d}r$$

For the three types of deformation follows:

Term	Part of U_b
w_1	0
w_2	$+\frac{\pi}{3}\frac{Et^3f^2}{c^2}$
w_3	$+\frac{\pi Et^3}{24}B^2\lambda^3c\left(3-\frac{1}{\lambda c}\right)$
$2w_2w_3$	$+\frac{8\pi fB\lambda}{c}\frac{Et^3}{24}\left(1-\frac{1}{\lambda c}\right)$

The "external" energy equals:

$$U_q=q\int_0^c(\tfrac{1}{2}w_1+w_2+w_3)2\pi r\,\mathrm{d}r$$

There will be a stable state of equilibrium, when the expression

$$U=U_m+U_b-U_q \tag{13}$$

becomes a minimum.

This minimum follows from the equations

$$\frac{\partial U}{\partial f} = 0 \qquad \text{and} \qquad \frac{\partial U}{\partial c} = 0 \tag{14}$$

When applying these two conditions the load q and the rise f can be determined for a given radius c of the snap-through area.

The minimum value of q that follows from $\partial q/\partial c = 0$ will give rise to the critical load.

The two equations (14) become:

$$\begin{aligned}
\frac{\partial U}{\partial f} = 0 = {} & \frac{7}{24}\pi E c^2\left(\frac{4f^3}{c^4} - \frac{6t^2}{c^2R} + \frac{2f}{R^2}\right) + \frac{\pi}{8}Et\frac{\alpha_1^2}{\lambda^2c^2}\left\{\frac{\alpha_1^2}{\lambda c^3}\left(1 - \frac{3}{\lambda c}\right) + \right. \\
& - \frac{3\alpha_1^2}{R\lambda c}\left(1 - \frac{2}{\lambda c}\right) + \frac{2tc}{\lambda R^2}\left(1 - \frac{1}{\lambda c}\right)\Big\} - \pi qfR - \frac{\pi qR\alpha_1}{2\lambda c}\left\{\frac{\alpha_1}{\lambda c}\left(1 - \frac{1}{2\lambda c}\right) + \right. \\
& \left. - \frac{1}{R\lambda^2}\left(1 - \frac{1}{\lambda c}\right)\right\} - \frac{3\pi}{2}\frac{Et\alpha_1}{\lambda^2c^3}\left\{\frac{2f^3\alpha_1}{c^2}\left(-1 + \frac{5}{2\lambda c}\right) - \frac{3}{2}\frac{\alpha_1 f^2}{R}\left(-1 + \frac{5}{2\lambda c}\right) + \right. \\
& \left. + \frac{c^2}{R}\left(\frac{3f^2}{c^2} - \frac{2f}{R}\right)\left(1 - \frac{3}{2\lambda c}\right)\right\} + \frac{\pi Et^3}{24}\left\{\frac{16f}{c^2} + \frac{\alpha_1}{R}\left(1 - \frac{1}{\lambda c}\right)\right\}
\end{aligned} \tag{15}$$

and

$$\begin{aligned}
\frac{\partial U}{\partial c} = 0 = {} & \frac{7}{24}\pi Etf^2\left(\frac{-2f^2}{c^3} + \frac{2c}{R^2}\right) + \frac{\pi}{8}Et\frac{\alpha_1^2 f^2}{\lambda^2}\left\{\frac{-5\alpha_1^2 f^2}{4\lambda c^6}\left(1 - \frac{18}{5\lambda c}\right) + \right. \\
& \left. + \frac{3\alpha_1 f}{\lambda Rc^4}\left(1 - \frac{8}{3\lambda c}\right) - \frac{1}{\lambda R^2c^2}\left(1 - \frac{2}{\lambda c}\right)\right\} + \frac{\pi qR\alpha_1^2 f^2}{2\lambda^2c^3}\left(1 - \frac{2}{3\lambda c}\right) - \frac{3}{2}\frac{\pi Et\alpha_1 f^2}{\lambda^3} \cdot \\
& \cdot\left[\frac{-2f}{c^3}\left\{\frac{\alpha_1 f}{2c^3}\left(-1 + \frac{5}{2\lambda c}\right) + \frac{1}{Rc}\left(1 - \frac{3}{\lambda c}\right)\right\} + \left(\frac{f}{c^2} - \frac{1}{R}\right)\left\{\frac{-3\alpha_1 f}{2c^4}\left(-1 + \frac{10}{3\lambda c}\right) + \right.\right. \\
& \left.\left. - \frac{1}{Rc^2}\left(1 - \frac{6}{\lambda c}\right)\right\}\right] + \frac{\pi}{24}Et^3\left\{\frac{-16f^2}{c^3} - \frac{8f\alpha}{R\lambda c^2} + \frac{\alpha_1^2\lambda}{R^2}\left(9c^2 - \frac{2c}{\lambda}\right)\right\} + \frac{\pi\alpha_1 q}{\lambda^2 R}\left(2c - \frac{1}{\lambda}\right)
\end{aligned} \tag{16}$$

Three symbols are substituted by writing:

$$\begin{aligned}
f &= \Phi t \\
c &= \Psi\sqrt{Rt} \\
q &= \gamma\frac{Et^2}{R^2}
\end{aligned} \tag{17}$$

If the equation (15)

$$\frac{\partial U}{\partial f} = 0 \quad \text{is multiplied by} \quad \frac{24R}{\pi E t^3}$$

and the equation (16)

$$\frac{\partial U}{\partial c} = 0 \quad \text{by} \quad \frac{24R^{3/2}}{\pi E t^{7/2}},$$

the two equations will read

$$\Phi^3\left\{28\Psi^3+3^{1/4}\alpha_1^4\left(1-\frac{3^{3/4}}{\Psi}\right)+16.3^{1/4}\cdot\alpha_1^2\left(1-\frac{5}{2.3^{1/4}\Psi}\right)\right\}+$$

$$+\Phi^2\left\{-42\Psi^5-3^{5/4}\cdot\alpha_1^3\Psi^2\left(1-\frac{2}{3^{1/4}\Psi}\right)+36.3^{1/4}\alpha_1^2\Psi^2\left(1-\frac{3}{2.3^{1/4}\Psi}\right)-36.3^{1/4}\alpha_1\Psi^2\right\}$$

$$+\Phi\left\{14\Psi^7+2.3^{1/4}\alpha_1^2\Psi^4\left(1-\frac{1}{3^{1/4}\Psi}\right)+2.4.3^{1/4}\alpha_1\Psi^4\left(1-\frac{3}{2.3^{1/4}\Psi}\right)+16\Psi^3\right\}+$$

$$-24\gamma\Phi\Psi^5-4.3^{1/2}\alpha_1\gamma\Psi^3\left\{\alpha_1\Phi\left(1-\frac{1}{2.3^{1/4}\Psi}\right)-\frac{\Psi}{3^{1/4}}3+2.3^{1/4}\Psi-\frac{1}{3^{1/4}\Psi}\right)\right\}+$$

$$+8\alpha_1\Psi^5\left(1+\frac{\Phi}{\Psi^2}\right)\left(1-\frac{1}{3^{1/4}\Psi}\right)+2.3^{1/4}\alpha_1^2\Psi^6\left(3-\frac{1}{3^{1/4}\Psi}\right)=0 \qquad (15a)$$

and

$$\Phi^4\left\{-14^3-3^{1/4}\cdot5\alpha_1^4\left(1-\frac{18}{5.3^{1/4}\Psi}\right)-6.3^{1/4}\alpha_1^2\left(5-\frac{15}{3^{1/4}\Psi}\right)\right\}+$$

$$+\Phi^3\left\{3^{5/4}\cdot\alpha_1^2\Psi^2\left(7-\frac{68}{3^{5/4}\Psi}\right)+36.3^{1/4}\cdot\alpha_1\Psi^2\left(1-\frac{4}{3^{1/4}\Psi}\right)\right\}+$$

$$+\Phi^2\left\{14\Psi^7-3^{1/4}\cdot\Psi^4\alpha_1^2\left(1-\frac{2}{3^{1/4}\Psi}\right)-12.3^{1/4}\cdot\alpha_1\Psi^4\left(1-\frac{6}{3^{1/4}\Psi}\right)-16\Psi^3\right\}+$$

$$+\Phi\left\{\frac{24}{3^{1/4}}\Psi^4+8\alpha_1\Psi^5\left(2+\frac{1}{3^{1/4}\Psi}\right)\right\}-3^{5/4}\cdot\alpha_1^2\Psi^8+2\alpha_1^2\Psi^7=0 \qquad (16a)$$

By inserting the values of Ψ in the equation $\partial U/\partial c = 0$ it is possible to calculate Φ for different values of α.

If the corresponding values of ψ, Φ and α are substituted in the equation $\partial U/\partial f = 0$, various values of γ can be determined.

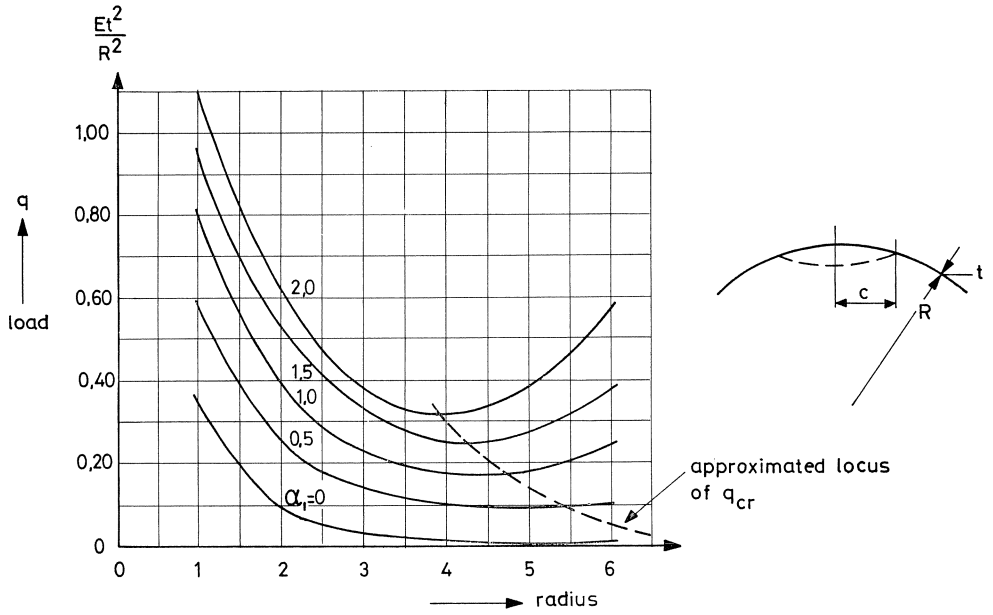

Fig. 19. The critical load q_{cr} as a function of the radius of the snap-through are.

The results of the calculations are shown in fig. 19. From it can be concluded that the snap-through area increases as the value of α_1 (or the rotational stiffness of the edge-beam) decreases.

When the load is increased to a critical value a snap-through area will appear in the vicinity of the edge. It will extend till c reaches the value for which there exists a stable equilibrium and q_{cr} is a minimum. In the case that the edge-beam has little rotational stiffness, then this value of q_{cr} will be relatively small.

Therefore shells with a shallow edge-beam and a rise f less than $20t$ – resulting in a value of α_1 between $0 < \alpha_1 < 0{,}50$ – will have a critical load less than $q_{cr} = 0.1Et^2/R^2$, as can be deducted from fig. 19. This fact explains the small values of q_{cr} resulting from some experiments. $f = 20t$ for $\alpha_1 = 1$.

If – on the other hand – there is a very stiff edge-beam, the value of α_1 will be large and the critical load may come to $q_{cr} = 0.32Et^2/R^2$. For shells with a small rise (e.g. $f < 20t$) a large part of the edge of the snap-through area will coincide with the edge-beam.

In this case the rotational stiffness of the edge-beam must be comparable with that of the edge in a continuous shell, so that $\alpha_1 = 1$. Then according to fig. 19,

$$q_{cr} = 0.2\frac{Et^2}{R^2}$$

Substituting edge-beam of similar stiffness

The dimensions of such an edge-beam can be calculated. A beam with a circular curved axis having a rectangular cross-section $B \times H$ subjected to a torsional moment m along the circumference will have an angle of rotation:

$$\varphi_b = \frac{mR^2 \sin^2 \vartheta}{EI} = \frac{12mR^2 \sin^2 \vartheta}{EBH^3} \tag{18}$$

if ϑ equals half the angle of aperture (fig. 20).

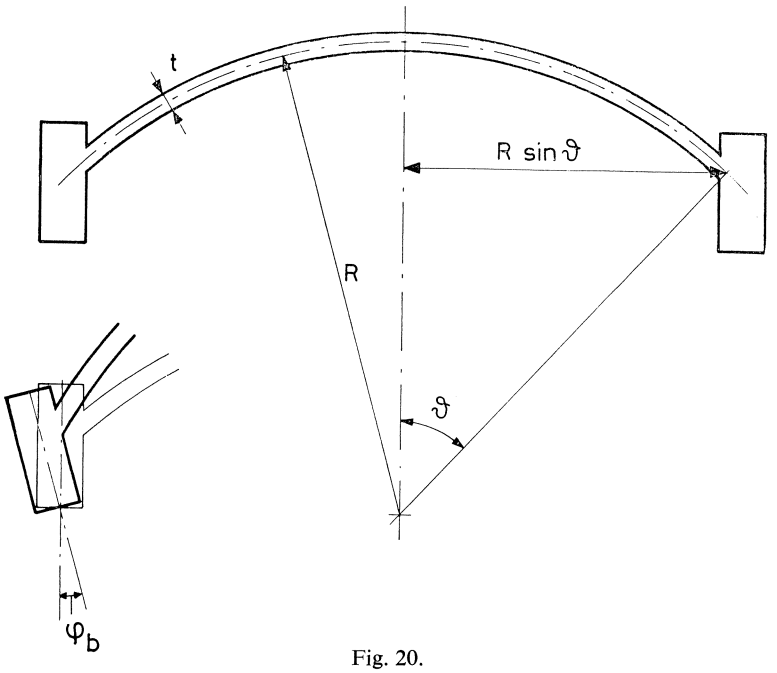

Fig. 20.

The slope of the shell due to a moment m can be calculated by equating "internal" and "external" energies:

$$\tfrac{1}{2}m\left(\frac{\mathrm{d}w}{\mathrm{d}r}\right)_c \cdot 2\pi c = \int_0^c \left\{\frac{Et^3}{24}\left(\frac{\mathrm{d}^2 w}{\mathrm{d}r^2}\right)^2 + \frac{1}{Et}\left(\frac{\mathrm{d}^2 \Phi}{\mathrm{d}r^2}\right)^2\right\} \cdot 2\pi r \,\mathrm{d}r$$

$$m = \frac{REt}{\alpha_1 c^2}\left[\frac{t^2}{24}\frac{\alpha_1^2 c^2}{R^2}\lambda c\left(3 - \frac{1}{\lambda c}\right) + \frac{\alpha_1^2 c^2}{8R^2\lambda^2}\left\{\tfrac{1}{4}\frac{\alpha_1^2}{\lambda^2 R^2}(\lambda c - 3) - \frac{\alpha_1 c}{\lambda R^2}\left(1 - \frac{2}{\lambda c}\right) + \right.\right.$$

$$\left.\left. + \frac{c}{\lambda R^2}\left(1 - \frac{1}{\lambda c}\right)\right\}\right] = \frac{Et^3}{24}\frac{\alpha_1}{R}\{6\lambda c - 4 + \tfrac{3}{4}\alpha_1^2(\lambda c - 3) - 3\alpha_1(\lambda c + 2)\}$$

Because $\lambda c \gg 1$ to approximate to:

$$m \approx \frac{Et^2\sqrt{3}}{32R} \cdot A(8-4\alpha_1+\alpha_1^2)$$

According to this formula:

$$\alpha_1 = 0, \quad m = \frac{Et^2}{2.3R}A$$

$$\alpha_1 = 1, \quad m = \frac{Et^2}{3.7R}A$$

$$\alpha_1 = 2, \quad m = \frac{Et^2}{4.6R}A$$

This result will be approximated in accordance with eq. (6):

$$m = \frac{Et^2}{3R}A \quad \text{for} \quad \varphi_s = \lambda A$$

Hence

$$\varphi_s = \lambda\frac{3Rm}{Et^2} = \frac{\sqrt[4]{3}}{\sqrt{Rt}}\frac{3Rm}{Et^2} \approx \frac{4\sqrt{Rt}}{Et^3}m \tag{19}$$

If the approximation of Geckeler is applied the value of φ_s equals:

$$\varphi_s = \frac{2.6\sqrt{Rt}}{Et^3}m, \quad \text{see e.g. [13]}$$

For

$$B = bt,$$

$$H = ht, \quad \text{and}$$

$\varphi_b = \varphi_s$ (thus $\alpha_1 = 1$) and applying the formula (18):

$$\varphi_b = \frac{12mR^2\sin^2\vartheta}{Et^4bh^3}$$

The result is:

$$4\frac{\sqrt{Rt}}{Et^3} = \frac{12R^2\sin^2\vartheta}{Et^4bh^3}$$

or

$$bh^3 = 3\left(\frac{R}{t}\right)^{3/2}\sin^2\vartheta \tag{20}$$

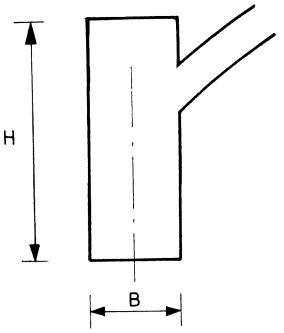

Fig. 21.

Using this formula, the edge-beam dimensions can be determined (fig. 21). If $b = h$ (or $B = H$) values for current relations of R/t are given in a table, rounded off in integers. When using this table it should be kept in mind that it has been derivated for $\alpha_1 = 1$

	$\vartheta = 10°$	$\vartheta = 30°$	$\vartheta = 60°$	$\vartheta = 90°$
$R/t = 100$	$B = H = 3t$	$5t$	$7t$	$7t$
$R/t = 500$	$6t$	$10t$	$12t$	$13t$
$R/t = 1000$	$7t$	$12t$	$16t$	$17t$

Numerical example

For a spherical shell having a radius of curvature $R = 1000$ cm, a thickness $t = 10$ cm and half the angle of aperture of 30° and a value of α_1 equals 1, $B \times H$ will be: $5t \times 5t$. In that case the edge-beam needs to have a cross-section of 50×50 cm.

For a rectangular cross-section the equivalent of $bh^3 = (5t)^4 = 625t^4$ should be chosen, for instance: $2t \times (6.8t)^3$ or $4t \times (5.4t)^3$ resulting in 20×68 cm resp. 40×54 cm.

Predicting the value of the critical load

The critical load can be predicted from fig. 19, if α_1 is expressed in terms of the dimensions of the edge-beam and the shell (fig. 20). From (5) and (11) follow:

$$\varphi_s = A\lambda = \alpha_1 \frac{c}{R} = \alpha_1 \sin\vartheta \approx \alpha_1 \vartheta$$

Hence

$$\alpha_1 = \frac{\varphi_s}{\vartheta}$$

φ_s is the angular rotation of the shell edge due to the edge disturbance. The angular

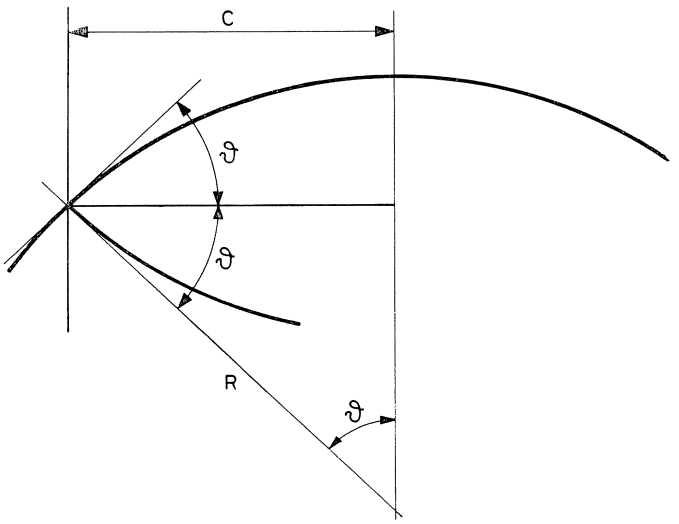

Fig. 22.

rotation of the shell edge and the edge beam together equals 2ϑ: $\varphi_s + \varphi_b = 2\vartheta$, as a result of the geometry of the mirroring effect (fig. 22).

Moreover one should be aware of the fact that in the derivation the final snap-through area and the area of the shell are taken to coincide.

Thus from (18) and (19):

$$\varphi_s = \frac{4\sqrt{Rt}}{Et^3} \frac{2\vartheta}{\frac{4\sqrt{Rt}}{Et^3} + \frac{12R^2\sin^2\vartheta}{EBH^3}}$$

and

$$\alpha_1 = \frac{2}{1 + \frac{3(R/t)^{3/2}t^4\sin^2\vartheta}{BH^3}} \quad \text{for} \quad \alpha_1 \leqq 2 \tag{21}$$

With the aid of this formula and using fig. 19 it will be possible to predict the critical load for a given shell.

As a numerical example is chosen the shell roof of the church St. Felix and Regula at Zürich (Switzerland) [14]. The shape of this shell is not quite a sphere; somewhat nearer to an ellipsoid.

However, the deviation is small and as was exposed in the preceding chapter II the difference in critical load will then be negligible.

The dimensions are approximately $2a_1 = 2400$ cm, $2b_1 = 1700$ cm, $f = 160$ cm. From this a minimum radius of 2200 cm on the basis of a circular vertical cross-section of the shell is determined.

$$t = 8 \text{ cm} \quad \text{and} \quad \frac{R}{t} = \frac{2200}{8} = 275$$

$$\vartheta = 20°$$

$$B = H = 30 \text{ cm, approximately } 4t$$

Substituted in formula (21):

$$\alpha = \frac{2}{1 + \dfrac{3 \times \left(\dfrac{2200}{8}\right)^{3/2} 8^4 \sin^2 20°}{30^4}} = \frac{2}{1+8.2} \sim 0.22$$

Indeed this value of α_1 is very small; it proves that the edge-beam does not appreciably resist to rotation. Furthermore, the rise of the shell is such that the circumference of the snap-through area coincides with the curved edge-beam.

From fig. 19 follows

$$q_{cr} \approx 0.055 \frac{Et^2}{R^2}$$

A test, carried out by Torroja-Schubiger [14] on a model resulted in a value of

$$q_{cr} = 0.069 \frac{Et^2}{R^2}$$

In addition: $\sqrt{Rt} = \sqrt{2200.8} \sim 133$ cm. The corresponding radius c will be: $c = 6\sqrt{Rt} = 6.133 \sim 800$ cm. The short axis of the ellips is $\frac{1}{2} \cdot 1700 = 850$ cm. After buckling it was found that the circumference of the snap-through area followed the edge-beam. This shows a fair agreement, taking into account the introduced approximations and simplifications.

Influence of crack formation

For concrete shells there is another phenomenon that may diminish the critical load. If cracks are so situated that they can influence the critical load, q_{cr} can be much less than hitherto described.

Tests made by Khaidukov [15] on doubly curved shells having rectangular edges gave rise to a crack pattern of concentric ellipses. The double curvature was far remote from the spherical shell, the ratio R_1/R_2 being about 16, so that the concept of a cylindrical shell in order to investigate buckling seems more appropriate.

The influence of cracking on the critical load of spherical shells has not been investi-

gated, although it is apparent that doubly curved shells of positive Gaussian curvature index will behave differently towards cracks than the single-curved ones. There exists a need for research into this subject.

Literature

1. Zoelly, Über ein Knickproblem an der Kugelschale, 1915. Dissertation, Zürich 1915.
2. Von Kármán and Tsien, The buckling of thin cylindrical shells under axial compression. Journ. Aeronautical Sciences 8, 1941.
3. Kempfer, Postbuckling behaviour of axially circular cylindrical shells. Journ. Aeronautical Sciences 21, 1954.
4. Ebner, Instabilitätserscheinungen bei dünwandige Baukörper, V.D.I. Zeitschrift, 1 Dec. 1962.
5. Wolmir, Biegsame Platten und Schalen, German Translation by Duda, 1962.
6. Mehmel, Einige Ergebnisse einer Modellstatische Untersuchung auf Durchschlagen, Proceedings Symposium on Shell Research, Delft 1962.
7. Schmidt, Ergebnisse von Beulversuchung auf doppelt gekrümmten Schalenmodellen, Proceedings Symposium on Shell Research, Delft 1962.
8. Von Kármán and Tsien, The buckling of spherical shells by external pressure. Journal of the Aeron. Sciences. Vol. 7, nr. 2, 1939.
9. Haas, Design of thin concrete shells, volume II, chapter XII, 1967, John Wiley, New York.
10. Van Koten and Haas, The stability of doubly curved surfaces having a positive Gaussian curvature index. Symposium I.A.S.S., Budapest, 1965. – Kultura 1967.
11. Pogorelov, Geometrical Methods in the Non-linear Theory of Shells. Theory of Thin Shells, Copenhagen 1967, Springer Verlag 1969.
12. Van Koten and Haas, The influence of the edge stiffness and the angle of aperture on the stability of a spherical shell. Congress I.A.S.S. Leningrad 1966 – Proceedings TSINIS, Moscow 1968.
13. Haas, Design of thin concrete shells, volume I, 1962, John Wiley, New York.
14. Torroja und Schubiger, Die Schalenkuppel in vorgespannter Beton der Kirche F. und R., Schw. Bauzeitung, 29 April 1950.
15. Khaidukov and Iskhakov, Research on models and calculation of shallow rectangular shells having a positive Gaussian curvature using limit design. Journal of Concrete and Reinforced Concrete, no. 1, Moscow 1966.